DE GRUYTER Comput. Methods Appl. Math. 2017; aop

Research Article

Max Gunzburger, Nan Jiang and Zhu Wang*

A Second-Order Time-Stepping Scheme for Simulating Ensembles of Parameterized Flow Problems

https://doi.org/10.1515/cmam-2017-0051
Received April 9, 2017; revised November 7, 2017; accepted November 9, 2017

Abstract: We consider settings for which one needs to perform multiple flow simulations based on the Navier–Stokes equations, each having different initial condition data, boundary condition data, forcing functions, and/or coefficients such as the viscosity. For such settings, we propose a second-order time accurate ensemble-based method that to simulate the whole set of solutions, requires, at each time step, the solution of only a single linear system with multiple right-hand-side vectors. Rigorous analyses are given proving the conditional stability and establishing error estimates for the proposed algorithm. Numerical experiments are provided that illustrate the analyses.

Keywords: Navier–Stokes Equations, Parameterized Flow, Ensemble Method

MSC 2010: 65M60, 76D05

1 Introduction

Many computational fluid dynamics applications require multiple simulations of a flow under different input conditions. For example, the ensemble Kalman filter approach used in data assimilation first simulates a forward model a large number of times by perturbing either the initial condition data, boundary condition data, or uncertain parameters, then corrects the model based on the model forecasts and observational data. A second example is the construction of low-dimensional surrogates for partial differential equation (PDE) solutions such as sparse-grid interpolants or proper orthogonal decomposition approximations, for which one has to first obtain expensive approximations of solutions corresponding to several parameter samples. Another example is sensitivity analyses of solutions for which one often has to determine approximate solutions for a number of perturbed inputs such as the values of certain physical parameters. In this paper, we consider such applications and develop a second-order time-stepping scheme for efficiently simulating an ensemble of flows. In particular, we consider the setting in which one wishes to determine the PDE solutions for several different choices of initial condition and boundary condition data, forcing functions, and physical parameters appearing in the PDE model.

The ensemble algorithm was first developed in [18] to find a set of J solutions of the Navier–Stokes equations (NSE) subject to different initial condition and forcing functions. The main idea is that, based on the

Max Gunzburger, Department of Scientific Computing, Florida State University, Tallahassee, FL 32306-4120, USA, e-mail: mgunzburger@fsu.edu
Nan Jiang, Department of Mathematics and Statistics, Missouri University of Science and Technology, Rolla, MO 65409-0020, USA, e-mail: jiangn@mst.edu
***Corresponding author: Zhu Wang,** Department of Mathematics, University of South Carolina, Columbia, SC 29208, USA, e-mail: wangzhu@math.sc.edu

introduction of an ensemble average and a special semi-implicit time discretization, the discrete systems for the multiple flow simulations share a common coefficient matrix. Thus, instead of solving J linear systems with J different matrices and right-hand sides, one only need solve a single linear system with J right-hand side vectors. This leads to very significant computational savings in linear solver costs when LU factorization (for small-scale systems) or a block iterative algorithm (for large-scale systems) are used. High-order ensemble algorithms were designed in [15, 16]. For high Reynolds number flows, ensemble regularization methods and a turbulence model based on ensemble averaging have been developed in [15, 17, 19, 24]. The method has also been extended to simulate MHD flows in [23] and to develop ensemble-based reduced-order modeling techniques in [8, 9]. In [10], the authors proposed a first-order ensemble algorithm that deals with a number of flow simulations subject to not only different initial condition, boundary conditions, and/or body force data, but also distinct viscosity coefficients appearing in the NSE model. In this paper, we follow the same direction and develop an ensemble scheme having higher accuracy.

To begin, consider an ensemble of incompressible flow simulations on a bounded domain subject to Dirichlet boundary conditions. The j-th member of the ensemble is a simulation associated with the positive viscosity coefficient ν_j, initial condition data u_j^0, boundary condition data g_j, and body force f_j. All of these data may vary from one simulation to another. Then, for $j = 1, \dots, J$, we need to solve

$$\begin{aligned} u_{j,t} + u_j \cdot \nabla u_j - \nu_j \Delta u_j + \nabla p_j &= f_j(x,t) && \text{in } \Omega \times [0,\infty), \\ \nabla \cdot u_j &= 0 && \text{in } \Omega \times [0,\infty), \\ u_j &= g_j(x,t) && \text{on } \partial\Omega, \\ u_j(x,0) &= u_j^0(x) && \text{in } \Omega. \end{aligned} \tag{1.1}$$

There is a long list of work in developing time discretization methods for the NSE including explicit, implicit, and semi-implicit schemes, for example, [11–14, 20, 22, 25]. In general, explicit schemes are easier to implement, but they suffer the severely restricted time step size from stability requirement. The fully implicit and semi-implicit schemes have better stability conditions, but the discretization would lead to a varying coefficient matrix of the system. As a result, a different linear system has to be solved for each member at every time step, thus totally J linear systems need to be solved per time step. To overcome this issue, we propose a new, second-order accurate in time, ensemble-based scheme that improves the computational efficiency. The scheme is semi-implicit that permits the use of a known quantity (the ensemble mean defined below), which is independent of the ensemble index j, in the advection term and, therefore, leads to a single coefficient matrix for all the ensemble members.

For keeping the exposition simple, we consider a uniform time step Δt and let $t_n = n\Delta t$ for $n = 0, 1, \dots$. We then consider the ensemble of semi-discrete in time systems

$$\begin{aligned} \frac{3u_j^{n+1} - 4u_j^n + u_j^{n-1}}{2\Delta t} + \overline{u}^n \cdot \nabla u_j^{n+1} + u_j'^{\,n} \cdot \nabla(2u_j^n - u_j^{n-1}) + \nabla p_j^{n+1} - \overline{\nu}\Delta u_j^{n+1} - (\nu_j - \overline{\nu})\Delta(2u_j^n - u_j^{n-1}) &= f_j^{n+1}, \\ \nabla \cdot u_j^{n+1} &= 0, \end{aligned} \tag{1.2}$$

where u_j^n, p_j^n and f_j^n denote approximations of $u_j(\cdot, t_n)$, $p_j(\cdot, t_n)$ and $f_j(\cdot, t_n)$ of (1.1), respectively. In (1.2), $\overline{u}^n$ and $\overline{\nu}$ denote the ensemble means of the velocity field and viscosity coefficient, respectively, defined by

$$\overline{u}^n := \frac{1}{J}\sum_{j=1}^{J}(2u_j^n - u_j^{n-1}) \quad \text{and} \quad \overline{\nu} := \frac{1}{J}\sum_{j=1}^{J}\nu_j$$

and $u_j'^{\,n}$ represents the fluctuation defined by

$$u_j'^{\,n} = 2u_j^n - u_j^{n-1} - \overline{u}^n.$$

It is easy to see that the coefficient matrix in the spatial discretization of (1.2) does not depend on j. Thus, all the members in the ensemble do share a common coefficient matrix. To advance one time step, one only need solve a single linear system with J right-hand side vectors, which is more efficient than solving J individual simulations.

We assume homogeneous flow boundary conditions ($g_j = 0$) in the following derivation and analysis of the proposed ensemble algorithm. But flows with inhomogeneous essential boundary conditions are considered in our first numerical experiment presented in Section 5, where, in the implementation, the data g_j at each time step is first replaced by its interpolant on the Lagrangian finite element space and then is enforced on the boundary nodes. The extension of our analysis to the inhomogeneous cases will follow the idea presented in [3], which will be discussed elsewhere.

In what follows, we present a rigorous theoretical analysis of the proposed scheme. In Section 2, we provide some notations and preliminaries; in Section 3, the stability conditions of the scheme are obtained; and in Section 4, an error estimate is derived. Then, several numerical experiments are presented in Section 5.

2 Notation and Preliminaries

Let Ω be an open, regular domain in $\mathbb{R}^d$ ($d = 2$ or 3). The space $L^2(\Omega)$ is equipped with the norm $\|\cdot\|$ and inner product $(\cdot,\cdot)$. Denote by $\|\cdot\|_{L^p}$ and $\|\cdot\|_{W_p^k}$, respectively, the norms for $L^p(\Omega)$ and the Sobolev space $W_p^k(\Omega)$. Let $H^k(\Omega)$ be the Sobolev space $W_2^k(\Omega)$ equipped with the norm $\|\cdot\|_k$. For functions $v(x,t)$ defined on $(0,T)$, we define $(1 \le m < \infty)$

$$\|v\|_{\infty,k} := \operatorname*{Ess\,Sup}_{[0,T]} \|v(t,\cdot)\|_k \quad \text{and} \quad \|v\|_{m,k} := \left(\int_0^T \|v(t,\cdot)\|_k^m \, dt \right)^{\frac{1}{m}}.$$

Given a time step Δt, let $v^n = v(t_n)$ and define the discrete norms

$$|||v|||_{\infty,k} = \max_{0 \le n \le N} \|v^n\|_k \quad \text{and} \quad |||v|||_{m,k} := \left(\sum_{n=0}^N \|v^n\|_k^m \Delta t \right)^{\frac{1}{m}}.$$

Denote by $H^{-1}(\Omega)$ the dual space of bounded linear functionals defined on

$$H_0^1(\Omega) = \{v \in H^1(\Omega) : v = 0 \text{ on } \partial\Omega\}.$$

A norm for $H^{-1}(\Omega)$ is given by

$$\|f\|_{-1} = \sup_{0 \ne v \in H_0^1(\Omega)} \frac{(f,v)}{\|\nabla v\|}.$$

We choose the velocity space X and pressure space Q to be

$$X := (H_0^1(\Omega))^d \quad \text{and} \quad Q := L_0^2(\Omega) = \left\{ q \in L^2(\Omega) : \int_\Omega q \, dx = 0 \right\}.$$

The space of weakly divergence free functions is then

$$V := \{v \in X : (\nabla \cdot v, q) = 0 \text{ for all } q \in Q\}.$$

A weak formulation of (1.1) reads: find $u_j : [0,T] \to X$ and $p_j : [0,T] \to Q$ for a.e. $t \in (0,T]$ satisfying, for $j = 1,\dots,J$,

$$\begin{aligned} (u_{j,t}, v) + (u_j \cdot \nabla u_j, v) + \nu_j(\nabla u_j, \nabla v) - (p_j, \nabla \cdot v) &= (f_j, v) && \text{for all } v \in X, \\ (\nabla \cdot u_j, q) &= 0 && \text{for all } q \in Q, \end{aligned}$$

with $u_j(x,0) = u_j^0(x)$.

For the spatial discretization, we use a finite element (FE) method. However, the results can be extended to many other variational methods without much difficulty. Denote by $X_h \subset X$ and $Q_h \subset Q$ the conforming velocity and pressure FE spaces on an edge to edge triangulation of Ω with h denoting the maximum diameter of the triangles. Assume that the pair of spaces (X_h, Q_h) satisfy the discrete inf-sup (or LBB$_h$) condition, that is required to guarantee the stability of FE approximations. We also assume that the FE spaces satisfy the following approximation properties [21]:

$$\inf_{v_h \in X_h} \|v - v_h\| \le Ch^{k+1}\|v\|_{k+1} \quad \text{for all } v \in [H^{k+1}(\Omega)]^d, \tag{2.1}$$

$$\inf_{v_h \in X_h} \|\nabla(v - v_h)\| \le Ch^{k}\|v\|_{k+1} \quad \text{for all } v \in [H^{k+1}(\Omega)]^d, \tag{2.2}$$

$$\inf_{q_h \in Q_h} \|q - q_h\| \le Ch^{s+1}\|q\|_{s+1} \quad \text{for all } q \in H^{s+1}(\Omega), \tag{2.3}$$

where the generic constant $C > 0$ is independent of the mesh size h. One example for which the LBB$_h$ stability condition is satisfied is the family of Taylor–Hood P^{s+1}-P^s element pairs (i.e., $k = s + 1$ in the definition of X_h), for $s \ge 1$ [7]. The discrete divergence free subspace of X_h is

$$V_h := \{v_h \in X_h : (\nabla \cdot v_h, q_h) = 0 \text{ for all } q_h \in Q_h\}.$$

We assume the mesh and FE spaces satisfy the following standard inverse inequality (typical for locally quasi-uniform meshes and standard FE spaces, see, e.g., [2]): for all $v_h \in X_h$,

$$h\|\nabla v_h\| \le C_{(inv)}\|v_h\|. \tag{2.4}$$

Define the explicitly skew-symmetric trilinear form

$$b^*(u, v, w) := \frac{1}{2}(u \cdot \nabla v, w) - \frac{1}{2}(u \cdot \nabla w, v)$$

that satisfies the bounds [21]

$$b^*(u, v, w) \le C(\Omega)(\|\nabla u\|\|u\|)^{\frac{1}{2}}\|\nabla v\|\|\nabla w\| \quad \text{for all } u, v, w \in X, \tag{2.5}$$

$$b^*(u, v, w) \le C(\Omega)\|\nabla u\|\|\nabla v\|(\|\nabla w\|\|w\|)^{\frac{1}{2}} \quad \text{for all } u, v, w \in X, \tag{2.6}$$

where $C(\Omega)$ is a constant depending on the domain. Denote the exact solution to (1.1) and the FE approximate solution to (2.7) at $t = t_n$ by u_j^n and $u_{j,h}^n$, respectively.

The fully discrete finite element discretization of (1.2) at t_{n+1} is as follows: given $u_{j,h}^n$, find $u_{j,h}^{n+1} \in X_h$ and $p_{j,h}^{n+1} \in Q_h$ satisfying

$$\begin{cases} \left(\dfrac{3u_{j,h}^{n+1} - 4u_{j,h}^n + u_{j,h}^{n-1}}{2\Delta t}, v_h\right) + b^*(\overline{u}_h^n, u_{j,h}^{n+1}, v_h) + b^*(2u_{j,h}^n - u_{j,h}^{n-1} - \overline{u}_h^n, 2u_{j,h}^n - u_{j,h}^{n-1}, v_h) \\ \qquad - (p_{j,h}^{n+1}, \nabla \cdot v_h) + \overline{\nu}(\nabla u_{j,h}^{n+1}, \nabla v_h) + (\nu_j - \overline{\nu})(\nabla(2u_{j,h}^n - u_{j,h}^{n-1}), \nabla v_h) = (f_j^{n+1}, v_h), \qquad v_h \in X_h, \\ (\nabla \cdot u_{j,h}^{n+1}, q_h) = 0, \qquad q_h \in Q_h. \end{cases} \tag{2.7}$$

This is a two-step method that requires $u_{j,h}^0$ and $u_{j,h}^1$ to start the time stepping; $u_{j,h}^0$ is determined by the initial condition and $u_{j,h}^1$ can be computed by the first-order ensemble algorithm developed by the authors in [10] (which is locally second-order accurate) or by using a standard, non-ensemble time-stepping method to compute each individual simulation at the very first time step. Compared to the second-order ensemble scheme developed in [15] for the NSEs without variations in the viscosity coefficient, the scheme (2.7) for parametrized flows introduces an additional average of the viscosity coefficients for the parameterized flow ensemble. As is shown in the next section, the deviation of the flow viscosity coefficients from the ensemble average will play an important role in the stability analysis of the scheme.

3 Stability Analysis

We begin by proving the conditional, nonlinear, long time stability of (2.7) under conditions on the time step and viscosity coefficient deviation: for any $j = 1, \dots, J$, there exist $0 \le \mu < 1$ and $0 < \epsilon \le 2 - 2\sqrt{\mu}$ such that

$$C\frac{\Delta t}{\overline{\nu} h}\|\nabla u_{j,h}'^{\,n}\|^2 \le \frac{(2 - 2\sqrt{\mu} - \epsilon)\sqrt{\mu}}{2(\sqrt{\mu} + \epsilon)}, \tag{3.1}$$

$$\frac{|\nu_j - \overline{\nu}|}{\overline{\nu}} \le \frac{\sqrt{\mu}}{3}, \tag{3.2}$$

where C denotes a generic constant depending on the domain and the minimum angle of the mesh.

Theorem 3.1 (Stability). *The ensemble scheme* (2.7) *is stable provided conditions* (3.1)–(3.2) *hold. In particular, for $j = 1, \dots, J$ and for any $N \geq 2$, we have*

$$
\begin{aligned}
&\frac{1}{4}(\|u_{j,h}^N\|^2 + \|2u_{j,h}^N - u_{j,h}^{N-1}\|^2) + \frac{1}{8}\sum_{n=1}^{N-1}\|u_{j,h}^{n+1} - 2u_{j,h}^n + u_{j,h}^{n-1}\|^2 + \bar{\nu}\Delta t\frac{\sqrt{\mu}+\epsilon}{2-\sqrt{\mu}}\Big(\frac{\sqrt{\mu}}{2}\frac{2+\epsilon}{\sqrt{\mu}+\epsilon} - \frac{3|\nu_j - \bar{\nu}|}{2\bar{\nu}}\Big)\|\nabla u_{j,h}^N\|^2\\
&\quad + \frac{\bar{\nu}\Delta t}{3}\frac{\sqrt{\mu}+\epsilon}{2-\sqrt{\mu}}\Big(\frac{\sqrt{\mu}}{2}\frac{2+\epsilon}{\sqrt{\mu}+\epsilon} - \frac{3|\nu_j - \bar{\nu}|}{2\bar{\nu}}\Big)\|\nabla u_{j,h}^{N-1}\|^2\\
&\leq \sum_{n=1}^{N-1}\frac{\sqrt{\mu}+\epsilon}{2\epsilon(2-\sqrt{\mu})}\frac{\Delta t}{\bar{\nu}}\|f_j^{n+1}\|_{-1}^2 + \frac{1}{4}(\|u_{j,h}^1\|^2 + \|2u_{j,h}^1 - u_{j,h}^0\|^2) + \bar{\nu}\Delta t\frac{\sqrt{\mu}+\epsilon}{2-\sqrt{\mu}}\Big(\frac{\sqrt{\mu}}{2}\frac{2+\epsilon}{\sqrt{\mu}+\epsilon} - \frac{3|\nu_j - \bar{\nu}|}{2\bar{\nu}}\Big)\|\nabla u_{j,h}^1\|^2\\
&\quad + \frac{\bar{\nu}\Delta t}{3}\frac{\sqrt{\mu}+\epsilon}{2-\sqrt{\mu}}\Big(\frac{\sqrt{\mu}}{2}\frac{2+\epsilon}{\sqrt{\mu}+\epsilon} - \frac{3|\nu_j - \bar{\nu}|}{2\bar{\nu}}\Big)\|\nabla u_{j,h}^0\|^2.
\end{aligned}
\tag{3.3}
$$

Proof. See Appendix A. □

Remark 3.2. Observe that the stability conditions (3.1) and (3.2) are oppositional to each other. The upper bound for the relative deviation of the viscosity coefficient given in (3.2) must be less than $\frac{\sqrt{\mu}}{3}$ whereas the upper bound in the time-step condition (3.1) must be less than $1 - \sqrt{\mu}$ because this bound is increasing when ϵ is decreasing, and it approaches $1 - \sqrt{\mu}$ as $\epsilon \to 0$. In practice, condition (3.2) is easy to check. If it does not hold, one could split the ensemble into smaller groups so that this condition holds for each group. Condition (3.1) can be satisfied by adjusting the time-step size.

4 Error Analysis

In this section we derive the numerical error estimate of the proposed ensemble scheme (2.7). We first give a lemma on the estimate of the consistency error of the backward differentiation formula that will be used in the error analysis for the fully discrete ensemble scheme.

Lemma 4.1. *For any $u \in H^3(0, T; L^2(\Omega))$, we have that*

$$
\Big\|\frac{3u^{n+1} - 4u^n + u^{n-1}}{2\Delta t} - u_t^{n+1}\Big\|^2 \leq \frac{7}{4}\Delta t^3\int_{t^{n-1}}^{t^{n+1}}\|u_{ttt}\|^2\,dt. \tag{4.1}
$$

Proof. The proof is given in Appendix B. □

By assuming that X_h and Q_h satisfy the LBB$_h$ condition, the ensemble scheme (2.7) is equivalent to: *for $n = 1, \dots, N-1$, find $u_{j,h}^{n+1} \in V_h$ such that*

$$
\begin{aligned}
&\Big(\frac{3u_{j,h}^{n+1} - 4u_{j,h}^n + u_{j,h}^{n-1}}{2\Delta t}, v_h\Big) + b^*(\bar{u}_h^n, u_{j,h}^{n+1}, v_h) + \bar{\nu}(\nabla u_{j,h}^{n+1}, \nabla v_h) + (\nu_j - \bar{\nu})(\nabla(2u_{j,h}^n - u_{j,h}^{n-1}), \nabla v_h)\\
&\quad + b^*(2u_{j,h}^n - u_{j,h}^{n-1} - \bar{u}_h^n, 2u_{j,h}^n - u_{j,h}^{n-1}, v_h) = (f_j^{n+1}, v_h), \quad v_h \in V_h.
\end{aligned}
\tag{4.2}
$$

To analyze the rate of convergence of the approximation, we assume the regularity assumptions on the NSE given by

$$
\begin{aligned}
&u_j \in H^2(0, T; H^{k+1}(\Omega)) \cap H^3(0, T; H^1(\Omega)),\\
&p_j \in L^2(0, T; H^{s+1}(\Omega)),\\
&f_j \in L^2(0, T; L^2(\Omega)).
\end{aligned}
$$

Let $e_j^n = u_j^n - u_{j,h}^n$ be the error between the true solution of (1.1) and the approximate solution determined from (4.2). We then have the following error estimates.

Theorem 4.2 (Error Estimate). *For any $j = 1, \dots, J$, under the stability conditions of* (3.1)–(3.2) *for some μ and ϵ satisfying $0 \leq \mu < 1$ and $0 < \epsilon \leq 2 - 2\sqrt{\mu}$, there exists a positive constant C independent of the time step Δt*

and mesh size h such that

$$\frac{1}{4}\|e_j^N\|^2 + C_1\overline{\nu}\Delta t\|\nabla e_j^N\|^2 \le e^{\frac{CT}{\overline{\nu}^3}}\bigg\{\frac{1}{4}(\|e_j^1\|^2 + \|2e_j^1 - e_j^0\|^2) + C_1\overline{\nu}\Delta t\|\nabla e_j^1\|^2 + C_2\overline{\nu}\Delta t\|\nabla e_j^0\|^2 + C\overline{\nu}^{-1}h^{2k}|||u_j|||_{4,k+1}^4$$
$$+ C\overline{\nu}^{-1}h^{2k} + C\Delta t^4\frac{|\nu_j - \overline{\nu}|^2}{\overline{\nu}}\|\nabla u_{j,tt}\|_{2,0}^2 + C\overline{\nu}^{-1}\Delta t^4\|u_{j,tt}\|_{2,0}^2 + C\overline{\nu}^{-1}h^{2k}|||u_j|||_{2,k+1}^2$$
$$+ Ch\Delta t^3\|\nabla u_{j,tt}\|_{2,0}^2 + Ch^{2k+1}\Delta t^3\|\nabla u_{j,tt}\|_{2,k+1}^2 + C\overline{\nu}^{-1}h^{2s+2}|||p_j|||_{2,s+1}^2$$
$$+ C\overline{\nu}^{-1}h^{2k+2}\|u_{j,t}\|_{2,k+1}^2 + C\overline{\nu}h^{2k}|||u_j|||_{2,k+1}^2 + C\frac{|\nu_j - \overline{\nu}|^2}{\overline{\nu}}h^{2k}|||u_j|||_{2,k+1}^2$$
$$+ C\overline{\nu}^{-1}\Delta t^4\|\nabla u_{j,ttt}\|_{2,0}^2\bigg\} + Ch^{2k+2}|||u_j|||_{\infty,k+1}^2 + C\overline{\nu}h^{2k}\Delta t|||u_j|||_{\infty,k+1}^2,$$

with positive constants

$$C_1 = 2C_0 + \frac{\sqrt{\mu} + \epsilon}{2 - \sqrt{\mu}}\Big(1 - 17C_0 - \frac{3|\nu_j - \overline{\nu}|}{2\overline{\nu}}\Big),$$
$$C_2 = C_0 + \frac{\sqrt{\mu} + \epsilon}{3(2 - \sqrt{\mu})}\Big(1 - 17C_0 - \frac{3|\nu_j - \overline{\nu}|}{2\overline{\nu}}\Big),$$
$$C_0 = \frac{1}{17}\frac{\epsilon}{\sqrt{\mu} + \epsilon}\Big(1 - \frac{\sqrt{\mu}}{2}\Big).$$

Proof. See Appendix C. □

It is well known that the Taylor–Hood P^{s+1}-P^s element pairs for which the LBB$_h$ stability condition and the approximation properties (2.1)–(2.3) are all satisfied [2, 7, 21]. In particular, when the popular P^2-P^1 Taylor–Hood FE is used (i.e., $k = 2$ and $s = 1$ in the definitions of X_h and Q_h, respectively), we have the following optimal convergence results.

Corollary 4.2.1. *Suppose the P^2-P^1 Taylor–Hood FE pair is used for the spatial discretization and assume that the initial errors $\|u_j^0 - u_{j,h}^0\|$, $\|\nabla(u_j^0 - u_{j,h}^0)\|$, $\|u_j^1 - u_{j,h}^1\|$ and $\|\nabla(u_j^1 - u_{j,h}^1)\|$ are all at least $O(h^2)$ accurate. Then the approximation error of the ensemble scheme* (2.7) *at time t_N satisfies*

$$\frac{1}{4}\|u_j^N - u_{j,h}^N\|^2 + 2C_0\overline{\nu}\Delta t\|\nabla(u_j^N - u_{j,h}^N)\|^2 \sim \mathcal{O}(h^4 + \Delta t^4 + h\Delta t^3).$$

5 Numerical Experiments

The goal of the numerical experiments is two-fold:

(i) to numerically illustrate the convergence rate of the ensemble algorithm (2.7), that is, illustrate the second-order accuracy in time.

(ii) to explore the stability of the algorithm.

In particular, the numerical results strongly indicate that the stability condition (3.2) is sharp.

5.1 Convergence Test

We illustrate the convergence rate of (2.7) by considering a test problem for the NSE from [6] that has an analytical solution. This solution preserves the spatial patterns of the Green–Taylor solution [1, 5] but the vortices do not decay as $t \to \infty$. On the unit square $\Omega = [0, 1]^2$, we define

$$u_{\mathrm{ref}} = [-s(t)\cos x\sin y, s(t)\sin x\cos y]^\top \quad \text{and} \quad p_{\mathrm{ref}} = -\frac{1}{4}[\cos(2x) + \cos(2y)]s^2(t)$$

with $s(t) = \sin(2t)$. We then have the corresponding source term

$$f_{\mathrm{ref}}(x, y, t) = (s'(t) + 2\nu s(t))[-\cos x\sin y, \sin x\cos y]^\top$$

and an inhomogeneous Dirichlet boundary condition with data $g_{\mathrm{ref}}^0(x, y, t) = u_{\mathrm{ref}}(x, y, t)$ for $(x, y) \in \partial\Omega$ and zero initial condition data $u_{\mathrm{ref}}^0(x, y) = u_{\mathrm{ref}}(x, y, 0) = [0, 0]^\top$.

To illustrate the convergence behavior, we consider an ensemble of two members with different viscosity coefficients and perturbed initial conditions. For the first member, we choose the viscosity coefficient $\nu_1 = 0.2$ and the exact solution is chosen as $u_1 = (1+\epsilon)u_{\text{ref}}$ whereas for the second member, we choose $\nu_2 = 0.3$ and $u_2 = (1-\epsilon)u_{\text{ref}}$, where $\epsilon = 10^{-3}$. The initial condition data, boundary condition data, and source terms are adjusted accordingly.

For this choice of parameters, we have $\frac{|\nu_j - \bar{\nu}|}{\bar{\nu}} = \frac{1}{5}$ for both $j = 1$ and $j = 2$; hence the stability condition (3.2) is satisfied. We first apply the ensemble algorithm (2.7) using the P^2-P^1 Taylor–Hood FE and evaluate the rates of convergence. The initial mesh size and time step size are chosen to be $h = 0.1$ and $\Delta t = 0.05$; both the spatial and temporal grids are uniformly refined. Numerical results are listed in Table 1 for which

$$\|\mathcal{E}_j^E\|_{\infty,0} = \max_{0\le n\le N} \|u_j^n - u_{j,h}^n\| \quad \text{and} \quad \|\nabla\mathcal{E}_j^E\|_{2,0} = \sqrt{\Delta t \sum_{n=0}^{N} \|\nabla(u_j^n - u_{j,h}^n)\|^2}.$$

It is seen that the convergence rates for both u_1 and u_2 are second order, which matches our theoretical analysis.

Furthermore, we implement the two individual simulations separately and denote the corresponding numerical errors by $\|\mathcal{E}_j^S\|_{\infty,0}$ and $\|\nabla\mathcal{E}_j^S\|_{2,0}$. Comparing the ensemble simulation solutions in Table 1 with the independent simulation results listed in Table 2, we observe that the former achieves the same order of accuracy as the latter.

Although the pressure error is not discussed in this paper, we determine the pressure approximation accuracy of the ensemble simulation using the same uniform mesh refinement strategy and then, in Table 3, provide results for $\|\mathcal{E}_{\mathcal{P}_j}^E\|_{\infty,0}$, the maximum values over all the time levels of the pressure errors in the L^2 norm. Results for approximate solutions obtained by the ensemble method as well as through separate computations are given. It is observed that the ensemble-based scheme achieves second-order convergence in the pressure approximation and the associated numerical errors are nearly identical to those obtained from individual simulations, $\|\mathcal{E}_{\mathcal{P}_j}^S\|_{\infty,0}$.

$\frac{1}{h}$	$\|\mathcal{E}_1^E\|_{\infty,0}$	rate	$\|\nabla\mathcal{E}_1^E\|_{2,0}$	rate	$\|\mathcal{E}_2^E\|_{\infty,0}$	rate	$\|\nabla\mathcal{E}_2^E\|_{2,0}$	rate
10	1.02e−04	–	8.51e−04	–	8.02e−05	–	7.99e−04	–
20	2.60e−05	1.98	2.12e−04	2.00	2.03e−05	1.98	1.99e−04	2.00
40	6.54e−06	1.99	5.31e−05	2.00	5.12e−06	1.99	4.99e−05	2.00
80	1.64e−06	1.99	1.33e−05	2.00	1.28e−06	2.00	1.25e−05	2.00

Table 1: Approximation errors for ensemble simulations of two members with inputs $\nu_1 = 0.2$, $u_1 = (1+10^{-3})u_{\text{ref}}$ and $\nu_2 = 0.3$, $u_2 = (1-10^{-3})u_{\text{ref}}$.

$\frac{1}{h}$	$\|\mathcal{E}_1^S\|_{\infty,0}$	rate	$\|\nabla\mathcal{E}_1^S\|_{2,0}$	rate	$\|\mathcal{E}_2^S\|_{\infty,0}$	rate	$\|\nabla\mathcal{E}_2^S\|_{2,0}$	rate
10	1.08e−04	–	8.79e−04	–	7.64e−05	–	7.79e−04	–
20	2.74e−05	1.98	2.20e−04	2.00	1.94e−05	1.98	1.94e−04	2.00
40	6.92e−06	1.99	5.50e−05	2.00	4.87e−06	1.99	4.85e−05	2.00
80	1.74e−06	1.99	1.38e−05	1.99	1.22e−06	2.00	1.21e−05	2.00

Table 2: Approximation errors for two individual simulations: $\nu_1 = 0.2$, $u_1 = (1+10^{-3})u_{\text{ref}}$ and $\nu_2 = 0.3$, $u_2 = (1-10^{-3})u_{\text{ref}}$.

$\frac{1}{h}$	$\|\mathcal{E}_{\mathcal{P}_1}^E\|_{\infty,0}$	rate	$\|\mathcal{E}_{\mathcal{P}_2}^E\|_{\infty,0}$	rate	$\|\mathcal{E}_{\mathcal{P}_1}^S\|_{\infty,0}$	rate	$\|\mathcal{E}_{\mathcal{P}_2}^S\|_{\infty,0}$	rate
10	2.09e−03	–	2.08e−03	–	2.08e−03	–	2.08e−03	–
20	5.27e−04	1.99	5.22e−04	1.99	5.27e−04	1.99	5.22e−04	1.99
40	1.32e−04	2.00	1.31e−04	1.99	1.32e−04	2.00	1.31e−04	1.99
80	3.30e−05	2.00	3.27e−05	2.00	3.30e−05	2.00	3.27e−05	2.00

Table 3: Pressure approximation errors for the ensemble and individual simulations.

5.2 Stability Tests

Two conditions, (3.1) and (3.2), guarantee the stability of the proposed scheme. Condition (3.2), in many applications, relates to the probability distribution of the uncertain physical parameters. This requirement on the parameter deviation ratio can be easily checked. If it is not fulfilled, one could divide the parameter sample set into smaller subsets so that it holds on each subset. Condition (3.1) depends on the nature of nonlinear problems. Its severity depends on the governing equations, domain, model parameters, initial/boundary conditions, forcing terms, etc. In practice, once condition (3.2) holds, condition (3.1) can be satisfied by making Δt sufficiently small and/or by dividing the ensemble into smaller ensembles. Of course, when the ensemble consists of high Reynolds number flows, this condition could easily fail due to the requirement of having an extremely small time-step size leading to a prohibitive computational cost. Condition (3.1) has been investigated extensively in [15, 18, 19]. Hence, in the following, we are mostly interested on the optimality of condition (3.2). However, we do consider the conditional stability due to (3.1) because we want to determine values of the parameter for which that condition is satisfied; this is not directly computable from (3.1) because of the generic constant appearing in that condition. Note that (3.2) contains no such constant so that we can directly study the sharpness of the condition.

We check the stability of our algorithm by using the problem of a flow between two offset circles (see, e.g., [15, 17–19]). The domain is a disk with a smaller off-center obstacle inside. By letting $r_1 = 1$, $r_2 = 0.1$, and $c = (c_1, c_2) = (\frac{1}{2}, 0)$, the domain is given by

$$\Omega = \{(x, y) : x^2 + y^2 \leq r_1^2 \text{ and } (x - c_1)^2 + (y - c_2)^2 \geq r_2^2\}.$$

The flow is driven by a counterclockwise rotational body force

$$f(x, y, t) = [-6y(1 - x^2 - y^2), 6x(1 - x^2 - y^2)]^\top \tag{5.1}$$

with no-slip boundary conditions imposed on both circles. A von Kármán vortex street forms behind the inner circle and then re-interacts with that circle and with itself, generating complex flow patterns. We consider multiple numerical simulations of the flow with different viscosity coefficients using the ensemble-based algorithm (2.7). For spatial discretization, we apply the P^2-P^1 Taylor–Hood element pair on a triangular mesh that is generated by a Delaunay triangulation with 80 mesh points on the outer circle and 60 mesh points on the inner circle and with refinement near the inner circle, resulting in 18,638 degrees of freedom; see Figure 1.

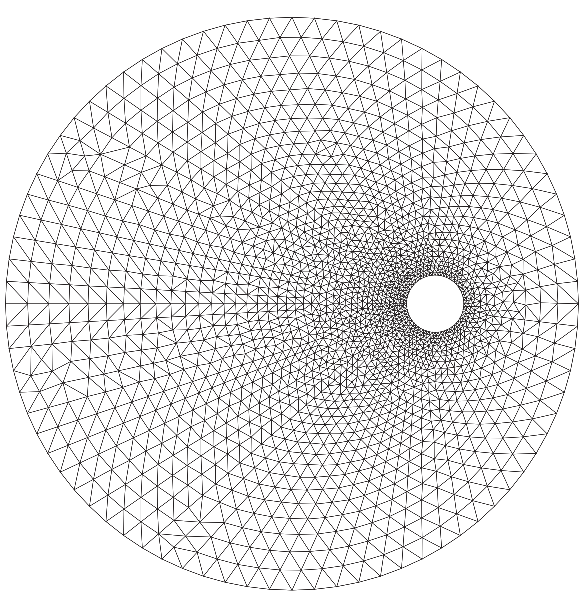

Figure 1: Mesh for the flow between two offset cylinders.

In order to illustrate the stability analysis based on conditions (3.1) and (3.2), we design two numerical tests involving two different sets of viscosity coefficients within an ensemble of three members, keeping the rest of computational setting, including the initial and boundary conditions and body force, the same for all the members. In particular, the initial condition is generated by solving the steady Stokes problem with viscosity $\nu = 0.03$ and the same body force $f(x, y, t)$ given by (5.1). We have two test cases:

- Case 1: $\nu_1 = 0.021$, $\nu_2 = 0.030$, $\nu_3 = 0.039$.
- Case 2: $\nu_1 = 0.019$, $\nu_2 = 0.030$, $\nu_3 = 0.041$.

Note that the viscosity coefficients ν_1 and ν_3 for Case 2 are obtained by making small perturbations from those for Case 1 with the average of the viscosity coefficients $\overline{\nu} = 0.03$ being the same for in both cases. However, the stability condition (3.2) holds in the first case but breaks down in the second case. In fact, the parameter deviation ratios are given by

- Case 1: $\frac{|\nu_1-\overline{\nu}|}{\overline{\nu}} = \frac{3}{10} < \frac{1}{3}$, $\frac{|\nu_2-\overline{\nu}|}{\overline{\nu}} = 0 < \frac{1}{3}$, $\frac{|\nu_3-\overline{\nu}|}{\overline{\nu}} = \frac{3}{10} < \frac{1}{3}$.
- Case 2: $\frac{|\nu_1-\overline{\nu}|}{\overline{\nu}} = \frac{11}{30} > \frac{1}{3}$, $\frac{|\nu_2-\overline{\nu}|}{\overline{\nu}} = 0 < \frac{1}{3}$, $\frac{|\nu_3-\overline{\nu}|}{\overline{\nu}} = \frac{11}{30} > \frac{1}{3}$.

For the stability test, we use the kinetic energy as a criterion and compare the ensemble simulation results to the independent simulations using the same mesh and time-step size.

Case 1. Condition (3.2) is satisfied so that this case illustrates the conditional stability due to (3.1). As mentioned above, we also use this test to determine a value for Δt for which (3.1) is satisfied so that, in Case 2, we can study the sharpness of condition (3.2). We first test the ensemble-based algorithm at a large time step size $\Delta t = 0.5$. The corresponding evolutions of the energy of all the three members are plotted in Figure 2. It is seen that for $\Delta t = 0.5$, the algorithm is unstable because the energy of the third member increases dramatically after $t = 4$ and that of the first member after $t = 4.5$. Although not shown in this figure, the energy of the second member also blows up but not until after $t = 20$. This implies that the stability condition (3.1) does not hold. Therefore, we next decrease the time step size to $\Delta t = 0.05$ and re-run the ensemble simulations. The associated evolutions of the energies are shown in Figure 2, indicating that the algorithm is now stable over the same time interval. Indeed, additional numerical experiments show that, for any time step size smaller than 0.05, the algorithm is always stable in Case 1 over a much longer time interval, for instance, [0, 50]. When an even smaller time step size $\Delta t = 0.01$ is selected, the comparison of the energy evolutions of ensemble-based simulations with the corresponding independent simulations over the time interval [0, 5] is given in Figures 3. The ensemble simulation is obviously stable and the output energy approximations are very close to those of the independent simulations.

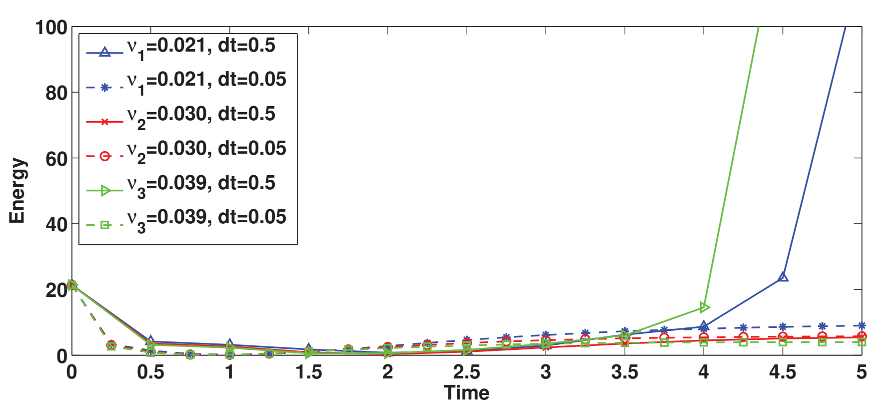

Figure 2: For the flow between two offset cylinders, Case 1, the energy evolution of the ensemble simulations for $\Delta t = 0.5$ and $\Delta t = 0.05$.

Case 2. We run ensemble simulations using the small time step size $\Delta t = 0.01$ over the same time interval as that for Case 1. As we mentioned above, the viscosity coefficients in Case 2 are obtained by slightly perturbing those in Case 1; this is the only difference between the two computational settings. Since Δt is chosen small, we believe condition (3.1) still holds for Case 2. But condition (3.2) no longer holds. Therefore, we expect

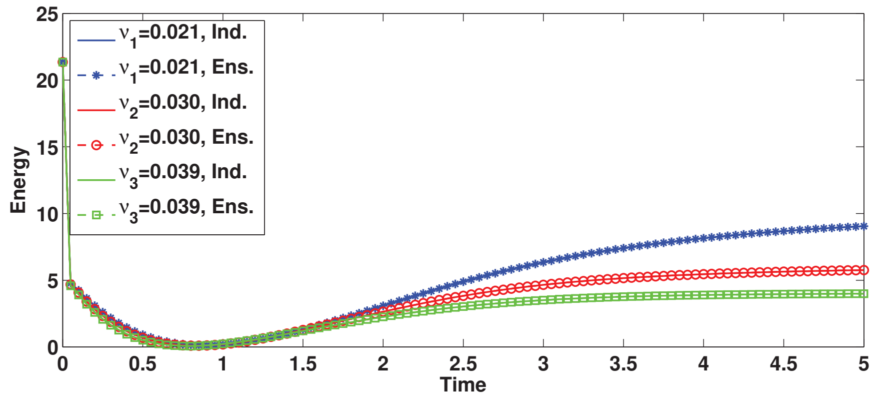

Figure 3: For the flow between two offset cylinders, Case 1, the energy evolution of the ensemble (Ens.) and independent simulations (Ind.) for $\Delta t = 0.01$.

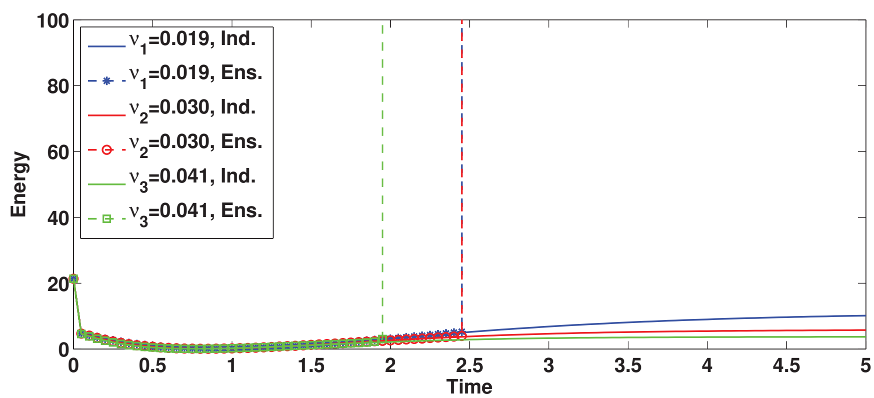

Figure 4: For the flow between two offset cylinders, Case 2, the energy evolution of the ensemble (Ens.) and independent simulations (Ind.) for $\Delta t = 0.01$.

the ensemble simulation to be unstable even when using the small time step size $\Delta t = 0.01$. The plots of energy evolutions in Figure 4 matches our expectation as they clearly indicate that the ensemble simulation is unstable in this case. In fact, the energy of the third member blows up after $t = 1.95$ and then affects the other two members and results in their energy dramatically increasing after $t = 2.45$.

6 Conclusions

In this paper, we develop a second-order time-stepping ensemble scheme to compute a set of Navier–Stokes equations in which every member is subject to an independent computational setting including a distinct viscosity coefficient, initial condition data, boundary condition data, and/or body force. By using the ensemble algorithm, all ensemble members share a common coefficient matrix after discretization, although with different right-hand side vectors. Therefore, many efficient block iterative solvers such as the block CG and block GMRES can be applied to solve such a single linear system with multiple right-hand side vectors, leading to great savings in both storage and simulation time. A rigorous analysis shows the proposed algorithm is conditionally, nonlinearly and long-time stable provided two explicit conditions hold and is second-order accurate in time. Two numerical experiments are presented that illustrate our theoretical analysis. In particular, the first is a test problem having an analytic solution that serves to illustrate that the rate of convergence with respect to the time-step size is indeed second order whereas the second example is for a flow between two offset cylinders and shows that the stability condition is sharp. For future work, we plan to investigate the performance of the ensemble algorithm in data assimilation applications.

A Proof of Theorem 3.1

Proof. Setting $v_h = u_{j,h}^{n+1}$ and $q_h = p_{j,h}^{n+1}$ in (2.7) and multiplying the result by Δt gives

$$\begin{aligned}\frac{1}{4}(\|u_{j,h}^{n+1}\|^2 + \|2u_{j,h}^{n+1} - u_{j,h}^n\|^2) - \frac{1}{4}(\|u_{j,h}^n\|^2 + \|2u_{j,h}^n - u_{j,h}^{n-1}\|^2) + \frac{1}{4}\|u_{j,h}^{n+1} - 2u_{j,h}^n + u_{j,h}^{n-1}\|^2 \\ + \bar{\nu}\Delta t\|\nabla u_{j,h}^{n+1}\|^2 + \Delta t b^*(2u_{j,h}^n - u_{j,h}^{n-1} - \overline{u}_h^n, 2u_{j,h}^n - u_{j,h}^{n-1}, u_{j,h}^{n+1}) \\ = \Delta t(f_j^{n+1}, u_{j,h}^{n+1}) - (\nu_j - \bar{\nu})\Delta t(\nabla(2u_{j,h}^n - u_{j,h}^{n-1}), \nabla u_{j,h}^{n+1}).\end{aligned}$$

Applying Young's inequality to the terms on the right-hand side yields, for any $\alpha, \beta_1, \beta_2 > 0$,

$$\begin{aligned}\frac{1}{4}(\|u_{j,h}^{n+1}\|^2 + \|2u_{j,h}^{n+1} - u_{j,h}^n\|^2) - \frac{1}{4}(\|u_{j,h}^n\|^2 + \|2u_{j,h}^n - u_{j,h}^{n-1}\|^2) + \frac{1}{4}\|u_{j,h}^{n+1} - 2u_{j,h}^n + u_{j,h}^{n-1}\|^2 \\ + \bar{\nu}\Delta t\|\nabla u_{j,h}^{n+1}\|^2 + \Delta t b^*(2u_{j,h}^n - u_{j,h}^{n-1} - \overline{u}_h^n, 2u_{j,h}^n - u_{j,h}^{n-1}, u_{j,h}^{n+1}) \\ \le \frac{\alpha\bar{\nu}\Delta t}{4}\|\nabla u_{j,h}^{n+1}\|^2 + \frac{\Delta t}{\alpha\bar{\nu}}\|f_j^{n+1}\|_{-1}^2 + \beta_1\bar{\nu}\Delta t\|\nabla u_{j,h}^{n+1}\|^2 + \frac{(\nu_j - \bar{\nu})^2\Delta t}{\beta_1\bar{\nu}}\|\nabla u_{j,h}^n\|^2 \\ + \frac{\beta_2\bar{\nu}\Delta t}{4}\|\nabla u_{j,h}^{n+1}\|^2 + \frac{(\nu_j - \bar{\nu})^2\Delta t}{\beta_2\bar{\nu}}\|\nabla u_{j,h}^{n-1}\|^2.\end{aligned} \tag{A.1}$$

Because the last four terms on the right-hand side of (A.1) need to be absorbed into $\bar{\nu}\Delta t\|\nabla u_{j,h}^{n+1}\|^2$ on the left-hand side, we minimize

$$\beta_1\bar{\nu}\Delta t\|\nabla u_{j,h}^{n+1}\|^2 + \frac{(\nu_j - \bar{\nu})^2\Delta t}{\beta_1\bar{\nu}}\|\nabla u_{j,h}^n\|^2$$

by taking $\beta_1 = \frac{|\nu_j - \bar{\nu}|}{\bar{\nu}}$ and

$$\frac{\beta_2\bar{\nu}\Delta t}{4}\|\nabla u_{j,h}^{n+1}\|^2 + \frac{(\nu_j - \bar{\nu})^2\Delta t}{\beta_2\bar{\nu}}\|\nabla u_{j,h}^{n-1}\|^2$$

by taking $\beta_2 = \frac{2|\nu_j - \bar{\nu}|}{\bar{\nu}}$. Then (A.1) becomes

$$\begin{aligned}\frac{1}{4}(\|u_{j,h}^{n+1}\|^2 + \|2u_{j,h}^{n+1} - u_{j,h}^n\|^2) - \frac{1}{4}(\|u_{j,h}^n\|^2 + \|2u_{j,h}^n - u_{j,h}^{n-1}\|^2) + \frac{1}{4}\|u_{j,h}^{n+1} - 2u_{j,h}^n + u_{j,h}^{n-1}\|^2 \\ + \bar{\nu}\Delta t\|\nabla u_{j,h}^{n+1}\|^2 + \Delta t b^*(2u_{j,h}^n - u_{j,h}^{n-1} - \overline{u}_h^n, 2u_{j,h}^n - u_{j,h}^{n-1}, u_{j,h}^{n+1}) \\ \le \frac{\alpha\bar{\nu}\Delta t}{4}\|\nabla u_{j,h}^{n+1}\|^2 + \frac{\Delta t}{\alpha\bar{\nu}}\|f_j^{n+1}\|_{-1}^2 + \frac{3|\nu_j - \bar{\nu}|\Delta t}{2}\|\nabla u_{j,h}^{n+1}\|^2 + |\nu_j - \bar{\nu}|\Delta t\|\nabla u_{j,h}^n\|^2 + \frac{|\nu_j - \bar{\nu}|\Delta t}{2}\|\nabla u_{j,h}^{n-1}\|^2.\end{aligned} \tag{A.2}$$

Next, we bound the trilinear term using inequality (2.6) and the inverse inequality (2.4):

$$\begin{aligned}&b^*(2u_{j,h}^n - u_{j,h}^{n-1} - \overline{u}_h^n, 2u_{j,h}^n - u_{j,h}^{n-1}, u_{j,h}^{n+1}) \\ &= b^*(2u_{j,h}^n - u_{j,h}^{n-1} - \overline{u}_h^n, -u_{j,h}^{n+1} + 2u_{j,h}^n - u_{j,h}^{n-1}, u_{j,h}^{n+1}) \\ &\le C\|\nabla(2u_{j,h}^n - u_{j,h}^{n-1} - \overline{u}_h^n)\|\|\nabla u_{j,h}^{n+1}\|\|\nabla(u_{j,h}^{n+1} - 2u_{j,h}^n + u_{j,h}^{n-1})\|^{\frac{1}{2}}\|u_{j,h}^{n+1} - 2u_{j,h}^n + u_{j,h}^{n-1}\|^{\frac{1}{2}} \\ &\le Ch^{-\frac{1}{2}}\|\nabla(2u_{j,h}^n - u_{j,h}^{n-1} - \overline{u}_h^n)\|\|\nabla u_{j,h}^{n+1}\|\|u_{j,h}^{n+1} - 2u_{j,h}^n + u_{j,h}^{n-1}\|.\end{aligned}$$

Using Young's inequality again gives

$$\begin{aligned}&\Delta t\big|b^*(2u_{j,h}^n - u_{j,h}^{n-1} - \overline{u}_h^n, 2u_{j,h}^n - u_{j,h}^{n-1}, u_{j,h}^{n+1})\big| \\ &\le C\frac{\Delta t^2}{h}\|\nabla(2u_{j,h}^n - u_{j,h}^{n-1} - \overline{u}_h^n)\|^2\|\nabla u_{j,h}^{n+1}\|^2 + \frac{1}{8}\|u_{j,h}^{n+1} - 2u_{j,h}^n + u_{j,h}^{n-1}\|^2.\end{aligned} \tag{A.3}$$

Substituting (A.3) into (A.2) and combining like terms, we have

$$\begin{aligned}\frac{1}{4}(\|u_{j,h}^{n+1}\|^2 + \|2u_{j,h}^{n+1} - u_{j,h}^n\|^2) - \frac{1}{4}(\|u_{j,h}^n\|^2 + \|2u_{j,h}^n - u_{j,h}^{n-1}\|^2) \\ + \frac{1}{8}\|u_{j,h}^{n+1} - 2u_{j,h}^n + u_{j,h}^{n-1}\|^2 + \bar{\nu}\Delta t\Big(1 - \frac{\alpha}{4} - \frac{3|\nu_j - \bar{\nu}|}{2\bar{\nu}}\Big)\|\nabla u_{j,h}^{n+1}\|^2 \\ \le \frac{\Delta t}{\alpha\bar{\nu}}\|f_j^{n+1}\|_{-1}^2 + C\frac{\Delta t^2}{h}\|\nabla(2u_{j,h}^n - u_{j,h}^{n-1} - \overline{u}_h^n)\|^2\|\nabla u_{j,h}^{n+1}\|^2 + |\nu_j - \bar{\nu}|\Delta t\|\nabla u_{j,h}^n\|^2 + \frac{|\nu_j - \bar{\nu}|\Delta t}{2}\|\nabla u_{j,h}^{n-1}\|^2.\end{aligned} \tag{A.4}$$

The second term on the right-hand side of (A.4), as well as the last two terms, need to be absorbed into the viscous term on the left-hand side. Thus we select an arbitrary number $\sigma \in (0,1)$, decompose the positive viscous term into four parts, and move all the terms that need to be bounded on right-hand side to the left-hand side of the inequality, which gives

$$\begin{aligned}
&\frac{1}{4}(\|u_{j,h}^{n+1}\|^2 + \|2u_{j,h}^{n+1} - u_{j,h}^{n}\|^2) - \frac{1}{4}(\|u_{j,h}^{n}\|^2 + \|2u_{j,h}^{n} - u_{j,h}^{n-1}\|^2)\\
&\quad + \frac{1}{8}\|u_{j,h}^{n+1} - 2u_{j,h}^{n} + u_{j,h}^{n-1}\|^2 + \bar{\nu}\Delta t\sigma\Big(1 - \frac{\alpha}{4} - \frac{3|\nu_j - \bar{\nu}|}{2\bar{\nu}}\Big)(\|\nabla u_{j,h}^{n+1}\|^2 - \|\nabla u_{j,h}^{n}\|^2)\\
&\quad + \bar{\nu}\Delta t\Big((1-\sigma)\Big(1 - \frac{\alpha}{4} - \frac{3|\nu_j - \bar{\nu}|}{2\bar{\nu}}\Big) - \frac{C\Delta t}{\bar{\nu}h}\|\nabla(2u_{j,h}^{n} - u_{j,h}^{n-1} - \bar{u}_h^{n})\|^2\Big)\|\nabla u_{j,h}^{n+1}\|^2\\
&\quad + \bar{\nu}\Delta t\Big(\frac{2}{3}\sigma\Big(1 - \frac{\alpha}{4} - \frac{3|\nu_j - \bar{\nu}|}{2\bar{\nu}}\Big) - \frac{|\nu_j - \bar{\nu}|}{\bar{\nu}}\Big)\|\nabla u_{j,h}^{n}\|^2\\
&\quad + \bar{\nu}\Delta t\frac{\sigma}{3}\Big(1 - \frac{\alpha}{4} - \frac{3|\nu_j - \bar{\nu}|}{2\bar{\nu}}\Big)(\|\nabla u_{j,h}^{n}\|^2 - \|\nabla u_{j,h}^{n-1}\|^2)\\
&\quad + \bar{\nu}\Delta t\Big(\frac{\sigma}{3}\Big(1 - \frac{\alpha}{4} - \frac{3|\nu_j - \bar{\nu}|}{2\bar{\nu}}\Big) - \frac{|\nu_j - \bar{\nu}|}{2\bar{\nu}}\Big)\|\nabla u_{j,h}^{n-1}\|^2\\
&\le \frac{\Delta t}{\alpha\bar{\nu}}\|f_j^{n+1}\|_{-1}^2.
\end{aligned} \tag{A.5}$$

Because $\alpha > 0$ is arbitrary, we take $\alpha = 4 - \frac{2(\sigma+1)}{\sigma}\sqrt{\mu}$. To make sure that α is greater than 0, we need

$$\sigma > \frac{\sqrt{\mu}}{2 - \sqrt{\mu}}, \quad \text{where } \frac{\sqrt{\mu}}{2 - \sqrt{\mu}} \in (0,1).$$

Now taking

$$\sigma = \frac{\sqrt{\mu} + \epsilon}{2 - \sqrt{\mu}}, \quad \text{where } \epsilon \in (0, 2 - 2\sqrt{\mu}),$$

inequality (A.5) becomes

$$\begin{aligned}
&\frac{1}{4}(\|u_{j,h}^{n+1}\|^2 + \|2u_{j,h}^{n+1} - u_{j,h}^{n}\|^2) - \frac{1}{4}(\|u_{j,h}^{n}\|^2 + \|2u_{j,h}^{n} - u_{j,h}^{n-1}\|^2) + \frac{1}{8}\|u_{j,h}^{n+1} - 2u_{j,h}^{n} + u_{j,h}^{n-1}\|^2\\
&\quad + \bar{\nu}\Delta t\sigma\Big(\frac{\sigma+1}{2\sigma}\sqrt{\mu} - \frac{3|\nu_j - \bar{\nu}|}{2\bar{\nu}}\Big)(\|\nabla u_{j,h}^{n+1}\|^2 - \|\nabla u_{j,h}^{n}\|^2)\\
&\quad + \bar{\nu}\Delta t\Big((1-\sigma)\Big(\frac{\sigma+1}{2\sigma}\sqrt{\mu} - \frac{3|\nu_j - \bar{\nu}|}{2\bar{\nu}}\Big) - \frac{C\Delta t}{\bar{\nu}h}\|\nabla(2u_{j,h}^{n} - u_{j,h}^{n-1} - \bar{u}_h^{n})\|^2\Big)\|\nabla u_{j,h}^{n+1}\|^2\\
&\quad + \bar{\nu}\Delta t\Big((\sigma+1)\Big(\frac{\sqrt{\mu}}{3} - \frac{|\nu_j - \bar{\nu}|}{\bar{\nu}}\Big)\Big)\|\nabla u_{j,h}^{n}\|^2\\
&\quad + \bar{\nu}\Delta t\frac{\sigma}{3}\Big(\frac{\sigma+1}{2\sigma}\sqrt{\mu} - \frac{3|\nu_j - \bar{\nu}|}{2\bar{\nu}}\Big)(\|\nabla u_{j,h}^{n}\|^2 - \|\nabla u_{j,h}^{n-1}\|^2)\\
&\quad + \bar{\nu}\Delta t\frac{\sigma+1}{2}\Big(\frac{\sqrt{\mu}}{3} - \frac{|\nu_j - \bar{\nu}|}{\bar{\nu}}\Big)\|\nabla u_{j,h}^{n-1}\|^2\\
&\le \frac{\Delta t}{\alpha\bar{\nu}}\|f_j^{n+1}\|_{-1}^2.
\end{aligned} \tag{A.6}$$

Stability follows if the following conditions hold:

$$\begin{aligned}
\frac{\sigma+1}{2\sigma}\sqrt{\mu} - \frac{3|\nu_j - \bar{\nu}|}{2\bar{\nu}} &\ge 0,\\
(1-\sigma)\Big(\frac{\sigma+1}{2\sigma}\sqrt{\mu} - \frac{3|\nu_j - \bar{\nu}|}{2\bar{\nu}}\Big) - \frac{C\Delta t}{\bar{\nu}h}\|\nabla(2u_{j,h}^{n} - u_{j,h}^{n-1} - \bar{u}_h^{n})\|^2 &\ge 0,\\
\frac{\sqrt{\mu}}{3} - \frac{|\nu_j - \bar{\nu}|}{\bar{\nu}} &\ge 0.
\end{aligned}$$

Under the assumption of (3.2), we have

$$\frac{\sqrt{\mu}}{3} - \frac{|\nu_j - \bar{\nu}|}{\bar{\nu}} \ge 0 \quad \text{and} \quad \frac{\sigma+1}{2\sigma}\sqrt{\mu} - \frac{3|\nu_j - \bar{\nu}|}{2\bar{\nu}} \ge \frac{\sqrt{\mu}(2 - \sqrt{\mu})}{2(\sqrt{\mu} + \epsilon)} \ge 0.$$

Together with the first assumption in (3.1), we have

$$
\begin{aligned}
(1-\sigma)\Big(\frac{\sigma+1}{2\sigma}\sqrt{\mu}-\frac{3|\nu_j-\overline{\nu}|}{2\overline{\nu}}\Big)&-\frac{C\Delta t}{\overline{\nu}h}\|\nabla(2u_{j,h}^n-u_{j,h}^{n-1}-\overline{u}_h^n)\|^2\\
&\geq\frac{(2-2\sqrt{\mu}-\epsilon)\sqrt{\mu}}{2(\sqrt{\mu}+\epsilon)}-\frac{C\Delta t}{\overline{\nu}h}\|\nabla(2u_{j,h}^n-u_{j,h}^{n-1}-\overline{u}_h^n)\|^2\\
&\geq\frac{(2-2\sqrt{\mu}-\epsilon)\sqrt{\mu}}{2(\sqrt{\mu}+\epsilon)}-\frac{(2-2\sqrt{\mu}-\epsilon)\sqrt{\mu}}{2(\sqrt{\mu}+\epsilon)}=0.
\end{aligned}
$$

Hence, we can draw the conclusion that the ensemble algorithm (2.7) is stable under conditions (3.1)–(3.2). Indeed, assuming both conditions (3.1)–(3.2) hold, (A.6) reduces to

$$
\begin{aligned}
\frac{1}{4}(\|u_{j,h}^{n+1}\|^2+\|2u_{j,h}^{n+1}-u_{j,h}^n\|^2)&-\frac{1}{4}(\|u_{j,h}^n\|^2+\|2u_{j,h}^n-u_{j,h}^{n-1}\|^2)+\frac{1}{8}\|u_{j,h}^{n+1}-2u_{j,h}^n+u_{j,h}^{n-1}\|^2\\
&+\overline{\nu}\Delta t\frac{\sqrt{\mu}+\epsilon}{2-\sqrt{\mu}}\Big(\frac{\sqrt{\mu}}{2}\frac{2+\epsilon}{\sqrt{\mu}+\epsilon}-\frac{3|\nu_j-\overline{\nu}|}{2\overline{\nu}}\Big)(\|\nabla u_{j,h}^{n+1}\|^2-\|\nabla u_{j,h}^n\|^2)\\
&+\frac{\overline{\nu}\Delta t}{3}\frac{\sqrt{\mu}+\epsilon}{2-\sqrt{\mu}}\Big(\frac{\sqrt{\mu}}{2}\frac{2+\epsilon}{\sqrt{\mu}+\epsilon}-\frac{3|\nu_j-\overline{\nu}|}{2\overline{\nu}}\Big)(\|\nabla u_{j,h}^n\|^2-\|\nabla u_{j,h}^{n-1}\|^2)\\
\leq\frac{\sqrt{\mu}+\epsilon}{2\epsilon(2-\sqrt{\mu})}\frac{\Delta t}{\overline{\nu}}\|f_j^{n+1}\|_{-1}^2.
\end{aligned}
\tag{A.7}
$$

Summing up (A.7) from $n=1$ to $N-1$ results in

$$
\begin{aligned}
\frac{1}{4}(\|u_{j,h}^N\|^2+\|2u_{j,h}^N-u_{j,h}^{N-1}\|^2)&+\frac{1}{8}\sum_{n=1}^{N-1}\|u_{j,h}^{n+1}-2u_{j,h}^n+u_{j,h}^{n-1}\|^2+\overline{\nu}\Delta t\frac{\sqrt{\mu}+\epsilon}{2-\sqrt{\mu}}\Big(\frac{\sqrt{\mu}}{2}\frac{2+\epsilon}{\sqrt{\mu}+\epsilon}-\frac{3|\nu_j-\overline{\nu}|}{2\overline{\nu}}\Big)\|\nabla u_{j,h}^N\|^2\\
&+\frac{\overline{\nu}\Delta t}{3}\frac{\sqrt{\mu}+\epsilon}{2-\sqrt{\mu}}\Big(\frac{\sqrt{\mu}}{2}\frac{2+\epsilon}{\sqrt{\mu}+\epsilon}-\frac{3|\nu_j-\overline{\nu}|}{2\overline{\nu}}\Big)\|\nabla u_{j,h}^{N-1}\|^2\\
\leq\sum_{n=1}^{N-1}\frac{\sqrt{\mu}+\epsilon}{2\epsilon(2-\sqrt{\mu})}\frac{\Delta t}{\overline{\nu}}\|f_j^{n+1}\|_{-1}^2&+\frac{1}{4}(\|u_{j,h}^1\|^2+\|2u_{j,h}^1-u_{j,h}^0\|^2)+\overline{\nu}\Delta t\frac{\sqrt{\mu}+\epsilon}{2-\sqrt{\mu}}\Big(\frac{\sqrt{\mu}}{2}\frac{2+\epsilon}{\sqrt{\mu}+\epsilon}-\frac{3|\nu_j-\overline{\nu}|}{2\overline{\nu}}\Big)\|\nabla u_{j,h}^1\|^2\\
&+\frac{\overline{\nu}\Delta t}{3}\frac{\sqrt{\mu}+\epsilon}{2-\sqrt{\mu}}\Big(\frac{\sqrt{\mu}}{2}\frac{2+\epsilon}{\sqrt{\mu}+\epsilon}-\frac{3|\nu_j-\overline{\nu}|}{2\overline{\nu}}\Big)\|\nabla u_{j,h}^0\|^2.
\end{aligned}
\tag{A.8}
$$

This completes the proof. □

B Proof of Lemma 4.1

Proof. To prove (4.1), we first rewrite

$$
\begin{aligned}
&3(u^{n+1}-u^n)-(u^n-u^{n-1})-2\Delta t u_t^{n+1}\\
&\quad=3\int_{t^n}^{t^{n+1}}u_t\,dt-\int_{t^{n-1}}^{t^n}u_t\,dt-2\Delta t u_t^{n+1}\\
&\quad=3\Big([(t-t^n)u_t]_{t^n}^{t^{n+1}}-\int_{t^n}^{t^{n+1}}(t-t^n)u_{tt}\,dt\Big)-\Big([(t-t^{n-1})u_t]_{t^{n-1}}^{t^n}-\int_{t^{n-1}}^{t^n}(t-t^{n-1})u_{tt}\,dt\Big)-2\Delta t u_t^{n+1}\\
&\quad=3\Delta t u_t^{n+1}-\Delta t u_t^n-2\Delta t u_t^{n+1}-3\int_{t^n}^{t^{n+1}}\frac{d}{dt}\Big(\frac{1}{2}(t-t^n)^2\Big)u_{tt}\,dt+\int_{t^{n-1}}^{t^n}\frac{d}{dt}\Big(\frac{1}{2}(t-t^{n-1})^2\Big)u_{tt}\,dt\\
&\quad=\Delta t u_t^{n+1}-\Delta t u_t^n-3\int_{t^n}^{t^{n+1}}\frac{d}{dt}\Big(\frac{1}{2}(t-t^n)^2\Big)u_{tt}\,dt+\int_{t^{n-1}}^{t^n}\frac{d}{dt}\Big(\frac{1}{2}(t-t^{n-1})^2\Big)u_{tt}\,dt
\end{aligned}
$$

$$
\begin{aligned}
&= \Delta t \int_{t^n}^{t^{n+1}} u_{tt}\,dt - 3\left(\left[\frac{1}{2}(t-t^n)^2 u_{tt}\right]_{t^n}^{t^{n+1}} - \int_{t^n}^{t^{n+1}} \frac{1}{2}(t-t^n)^2 u_{ttt}\,dt\right) \\
&\quad + \left(\left[\frac{1}{2}(t-t^{n-1})^2 u_{tt}\right]_{t^{n-1}}^{t^n} - \int_{t^{n-1}}^{t^n} \frac{1}{2}(t-t^{n-1})^2 u_{ttt}\,dt\right) \\
&= \Delta t\left([(t-t^n)u_{tt}]_{t^n}^{t^{n+1}} - \int_{t^n}^{t^{n+1}} (t-t^n)u_{ttt}\,dt\right) - 3\left(\frac{1}{2}\Delta t^2 u_{tt}^{n+1} - \int_{t^n}^{t^{n+1}} \frac{1}{2}(t-t^n)^2 u_{ttt}\,dt\right) \\
&\quad + \left(\frac{1}{2}\Delta t^2 u_{tt}^n - \int_{t^{n-1}}^{t^n} \frac{1}{2}(t-t^{n-1})^2 u_{ttt}\,dt\right) \\
&= \left(\Delta t^2 u_{tt}^{n+1} - \Delta t \int_{t^n}^{t^{n+1}} (t-t^n)u_{ttt}\,dt\right) - 3\left(\frac{1}{2}\Delta t^2 u_{tt}^{n+1} - \int_{t^n}^{t^{n+1}} \frac{1}{2}(t-t^n)^2 u_{ttt}\,dt\right) \\
&\quad + \left(\frac{1}{2}\Delta t^2 u_{tt}^n - \int_{t^{n-1}}^{t^n} \frac{1}{2}(t-t^{n-1})^2 u_{ttt}\,dt\right) \\
&= -\frac{1}{2}\Delta t^2(u_{tt}^{n+1} - u_{tt}^n) - \Delta t \int_{t^n}^{t^{n+1}} (t-t^n)u_{ttt}\,dt + 3\int_{t^n}^{t^{n+1}} \frac{1}{2}(t-t^n)^2 u_{ttt}\,dt - \int_{t^{n-1}}^{t^n} \frac{1}{2}(t-t^{n-1})^2 u_{ttt}\,dt \\
&= -\frac{1}{2}\Delta t^2 \int_{t^n}^{t^{n+1}} u_{ttt}\,dt - \Delta t \int_{t^n}^{t^{n+1}} (t-t^n)u_{ttt}\,dt + 3\int_{t^n}^{t^{n+1}} \frac{1}{2}(t-t^n)^2 u_{ttt}\,dt - \int_{t^{n-1}}^{t^n} \frac{1}{2}(t-t^{n-1})^2 u_{ttt}\,dt.
\end{aligned}
$$

Then the L^2 norm of the term of interest can be estimated as follows:

$$
\begin{aligned}
&\left\|\frac{3u^{n+1} - 4u^n + u^{n-1}}{2\Delta t} - u_t^{n+1}\right\|^2 \\
&= \frac{1}{4\Delta t^2}\int_\Omega \left|-\frac{1}{2}\Delta t^2 \int_{t^n}^{t^{n+1}} u_{ttt}\,dt - \Delta t \int_{t^n}^{t^{n+1}} (t-t^n)u_{ttt}\,dt + 3\int_{t^n}^{t^{n+1}} \frac{1}{2}(t-t^n)^2 u_{ttt}\,dt - \int_{t^{n-1}}^{t^n} \frac{1}{2}(t-t^{n-1})^2 u_{ttt}\,dt\right|^2 dx \\
&\le \frac{1}{2\Delta t^2}\int_\Omega \left(\frac{1}{4}\Delta t^4 \left|\int_{t^n}^{t^{n+1}} u_{ttt}\,dt\right|^2 + \Delta t^2 \left|\int_{t^n}^{t^{n+1}} (t-t^n)u_{ttt}\,dt\right|^2 + \frac{9}{4}\left|\int_{t^n}^{t^{n+1}} (t-t^n)^2 u_{ttt}\,dt\right|^2\right. \\
&\qquad \left. + \frac{1}{4}\left|\int_{t^{n-1}}^{t^n} (t-t^{n-1})^2 u_{ttt}\,dt\right|^2\right) dx \\
&\le \frac{1}{2\Delta t^2}\int_\Omega \left(\frac{1}{4}\Delta t^4 \left|\int_{t^n}^{t^{n+1}} u_{ttt}\,dt\right|^2 + \Delta t^4 \left[\int_{t^n}^{t^{n+1}} |u_{ttt}|\,dt\right]^2 + \frac{9}{4}\Delta t^4 \left[\int_{t^n}^{t^{n+1}} |u_{ttt}|\,dt\right]^2 + \frac{1}{4}\Delta t^4 \left[\int_{t^{n-1}}^{t^n} |u_{ttt}|\,dt\right]^2\right) dx \\
&\le \frac{1}{2\Delta t^2}\int_\Omega \left(\frac{1}{4}\Delta t^5 \int_{t^n}^{t^{n+1}} |u_{ttt}|^2\,dt + \Delta t^5 \int_{t^n}^{t^{n+1}} |u_{ttt}|^2\,dt + \frac{9}{4}\Delta t^5 \int_{t^n}^{t^{n+1}} |u_{ttt}|^2\,dt + \frac{1}{4}\Delta t^5 \int_{t^{n-1}}^{t^n} |u_{ttt}|^2\,dt\right) dx \\
&\le \frac{7}{4}\Delta t^3 \int_\Omega \int_{t^{n-1}}^{t^{n+1}} |u_{ttt}|^2\,dt\,dx \\
&\le \frac{7}{4}\Delta t^3 \int_{t^{n-1}}^{t^{n+1}} \|u_{ttt}\|^2\,dt.
\end{aligned}
$$

This completes the proof. □

C Proof of Theorem 4.2

Proof. The true solution (u_j, p_j) of the NSE satisfies

$$\Big(\frac{3u_j^{n+1}-4u_j^n+u_j^{n-1}}{2\Delta t}, v_h\Big) + b^*(u_j^{n+1}, u_j^{n+1}, v_h) + \nu_j(\nabla u_j^{n+1}, \nabla v_h) - (p_j^{n+1}, \nabla\cdot v_h)$$
$$= (f_j^{n+1}, v_h) + \mathrm{Intp}(u_j^{n+1}; v_h) \quad \text{for all } v_h \in V_h, \tag{C.1}$$

where $\mathrm{Intp}(u_j^{n+1}; v_h)$ is defined as

$$\mathrm{Intp}(u_j^{n+1}; v_h) = \Big(\frac{3u_j^{n+1}-4u_j^n+u_j^{n-1}}{2\Delta t} - u_{j,t}(t^{n+1}), v_h\Big).$$

Let

$$e_j^n = u_j^n - u_{j,h}^n = (u_j^n - I_h u_j^n) + (I_h u_j^n - u_{j,h}^n) = \eta_j^n + \xi_{j,h}^n,$$

where $I_h u_j^n \in V_h$ is the FE interpolant of u_j^n in V_h. Subtracting (4.2) from (C.1) gives

$$\Big(\frac{3\xi_{j,h}^{n+1}-4\xi_{j,h}^n+\xi_{j,h}^{n-1}}{2\Delta t}, v_h\Big) + b^*(u_j^{n+1}, u_j^{n+1}, v_h) + \bar\nu(\nabla\xi_{j,h}^{n+1}, \nabla v_h) + (\nu_j-\bar\nu)(\nabla(2\xi_{j,h}^n - \xi_{j,h}^{n-1}), \nabla v_h)$$
$$- b^*(2u_{j,h}^n - u_{j,h}^{n-1} - u_{j,h}'^n, u_{j,h}^{n+1}, v_h) - b^*(u_{j,h}'^n, 2u_{j,h}^n - u_{j,h}^{n-1}, v_h) - (p_j^{n+1}, \nabla\cdot v_h)$$
$$= -\Big(\frac{3\eta_j^{n+1}-4\eta_j^n+\eta_j^{n-1}}{2\Delta t}, v_h\Big) - \bar\nu(\nabla\eta_j^{n+1}, \nabla v_h) + \mathrm{Intp}(u_j^{n+1}; v_h) + (\bar\nu-\nu_j)(\nabla(2\eta_j^n - \eta_j^{n-1}), \nabla v_h)$$
$$+ (\bar\nu-\nu_j)(\nabla(u_j^{n+1} - 2u_j^n + u_j^{n-1}), \nabla v_h).$$

Setting $v_h = \xi_{j,h}^{n+1} \in V_h$ and rearranging the nonlinear terms leads to

$$\frac{1}{4\Delta t}(\|\xi_{j,h}^{n+1}\|^2 + \|2\xi_{j,h}^{n+1} - \xi_{j,h}^n\|^2) - \frac{1}{4\Delta t}(\|\xi_{j,h}^n\|^2 + \|2\xi_{j,h}^n - \xi_{j,h}^{n-1}\|^2) + \frac{1}{4\Delta t}\|\xi_{j,h}^{n+1} - 2\xi_{j,h}^n + \xi_{j,h}^{n-1}\|^2 + \bar\nu\|\nabla\xi_{j,h}^{n+1}\|^2$$
$$= -b^*(u_j^{n+1}, u_j^{n+1}, \xi_{j,h}^{n+1}) + b^*(2u_{j,h}^n - u_{j,h}^{n-1}, u_{j,h}^{n+1}, \xi_{j,h}^{n+1}) + b^*(u_{j,h}'^n, 2u_{j,h}^n - u_{j,h}^{n-1} - u_{j,h}^{n+1}, \xi_{j,h}^{n+1})$$
$$+ (p_j^{n+1}, \nabla\cdot\xi_{j,h}^{n+1}) - \Big(\frac{3\eta_j^{n+1}-4\eta_j^n+\eta_j^{n-1}}{2\Delta t}, \xi_{j,h}^{n+1}\Big) - \bar\nu(\nabla\eta_j^{n+1}, \nabla\xi_{j,h}^{n+1}) + \mathrm{Intp}(u_j^{n+1}; \xi_{j,h}^{n+1})$$
$$+ (\bar\nu-\nu_j)(\nabla(2\xi_{j,h}^n - \xi_{j,h}^{n-1}), \nabla\xi_{j,h}^{n+1}) + (\bar\nu-\nu_j)(\nabla(2\eta_j^n - \eta_j^{n-1}), \nabla\xi_{j,h}^{n+1})$$
$$+ (\bar\nu-\nu_j)(\nabla(u_j^{n+1} - 2u_j^n + u_j^{n-1}), \nabla\xi_{j,h}^{n+1}). \tag{C.2}$$

We first bound the viscous terms on the right-hand side of (C.2):

$$-(\nu_j-\bar\nu)(\nabla(u_j^{n+1} - 2u_j^n + u_j^{n-1}), \nabla\xi_{j,h}^{n+1}) \le \frac{1}{4C_0}\frac{|\nu_j-\bar\nu|^2}{\bar\nu}\|\nabla(u_j^{n+1} - 2u_j^n + u_j^{n-1})\|^2 + C_0\bar\nu\|\nabla\xi_{j,h}^{n+1}\|^2$$
$$\le \frac{\Delta t^3}{4C_0}\frac{|\nu_j-\bar\nu|^2}{\bar\nu}\int_{t^{n-1}}^{t^{n+1}}\|\nabla u_{j,tt}\|^2\,dt + C_0\bar\nu\|\nabla\xi_{j,h}^{n+1}\|^2, \tag{C.3}$$

and

$$-\bar\nu(\nabla\eta_j^{n+1}, \nabla\xi_{j,h}^{n+1}) \le \frac{\bar\nu}{4C_0}\|\nabla\eta_j^{n+1}\|^2 + C_0\bar\nu\|\nabla\xi_{j,h}^{n+1}\|^2, \tag{C.4}$$

$$-2(\nu_j-\bar\nu)(\nabla\eta_j^n, \nabla\xi_{j,h}^{n+1}) \le \frac{1}{C_0}\frac{|\nu_j-\bar\nu|^2}{\bar\nu}\|\nabla\eta_j^n\|^2 + C_0\bar\nu\|\nabla\xi_{j,h}^{n+1}\|^2, \tag{C.5}$$

$$(\nu_j-\bar\nu)(\nabla\eta_j^{n-1}, \nabla\xi_{j,h}^{n+1}) \le \frac{1}{4C_0}\frac{|\nu_j-\bar\nu|^2}{\bar\nu}\|\nabla\eta_j^{n-1}\|^2 + C_0\bar\nu\|\nabla\xi_{j,h}^{n+1}\|^2, \tag{C.6}$$

$$-2(\nu_j-\bar\nu)(\nabla\xi_{j,h}^n, \nabla\xi_{j,h}^{n+1}) \le \frac{1}{C_1}\frac{|\nu_j-\bar\nu|^2}{\bar\nu}\|\nabla\xi_{j,h}^n\|^2 + C_1\bar\nu\|\nabla\xi_{j,h}^{n+1}\|^2 \le |\nu_j-\bar\nu|\|\nabla\xi_{j,h}^n\|^2 + |\nu_j-\bar\nu|\|\nabla\xi_{j,h}^{n+1}\|^2, \tag{C.7}$$

$$(\nu_j-\bar\nu)(\nabla\xi_{j,h}^{n-1}, \nabla\xi_{j,h}^{n+1}) \le \frac{1}{4C_2}\frac{|\nu_j-\bar\nu|^2}{\bar\nu}\|\nabla\xi_{j,h}^{n-1}\|^2 + C_2\bar\nu\|\nabla\xi_{j,h}^{n+1}\|^2 \le \frac{|\nu_j-\bar\nu|}{2}\|\nabla\xi_{j,h}^{n-1}\|^2 + \frac{|\nu_j-\bar\nu|}{2}\|\nabla\xi_{j,h}^{n+1}\|^2, \tag{C.8}$$

where, because the terms on the right-hand side of (C.7) and (C.8) need to be hidden on the left-hand side of the error equation, we took $C_1 = \frac{|\nu_j-\bar\nu|}{\nu}$ and $C_2 = \frac{|\nu_j-\bar\nu|}{2\nu}$ in order to minimize their summations.

Next, we analyze the nonlinear terms on the right-hand side of (C.2) one by one. The first two nonlinear terms can be rewritten as

$$\begin{aligned} &-b^*(u_j^{n+1}, u_j^{n+1}, \xi_{j,h}^{n+1}) + b^*(2u_{j,h}^n - u_{j,h}^{n-1}, u_{j,h}^{n+1}, \xi_{j,h}^{n+1}) \\ &\quad = -b^*(2e_j^n - e_j^{n-1}, u_j^{n+1}, \xi_{j,h}^{n+1}) - b^*(2u_{j,h}^n - u_{j,h}^{n-1}, e^{n+1}, \xi_{j,h}^{n+1}) - b^*(u_j^{n+1} - 2u_j^n + u_j^{n-1}, u_j^{n+1}, \xi_{j,h}^{n+1}) \\ &\quad = -b^*(2\eta_j^n - \eta_j^{n-1}, u_j^{n+1}, \xi_{j,h}^{n+1}) - b^*(2\xi_{j,h}^n - \xi_{j,h}^{n-1}, u_j^{n+1}, \xi_{j,h}^{n+1}) - b^*(2u_{j,h}^n - u_{j,h}^{n-1}, \eta_j^{n+1}, \xi_{j,h}^{n+1}) \\ &\qquad - b^*(u_j^{n+1} - (2u_j^n - u_j^{n-1}), u_j^{n+1}, \xi_{j,h}^{n+1}). \end{aligned} \tag{C.9}$$

and

$$\begin{aligned} -b^*(2\eta_j^n - \eta_j^{n-1}, u_j^{n+1}, \xi_{j,h}^{n+1}) &\le C\|\nabla(2\eta_j^n - \eta_j^{n-1})\|\|\nabla u_j^{n+1}\|\|\nabla \xi_{j,h}^{n+1}\| \\ &\le C_0\overline{\nu}\|\nabla \xi_{j,h}^{n+1}\|^2 + \frac{C^2}{4C_0\overline{\nu}}(\|\nabla \eta_j^n\|^2 + \|\nabla \eta_j^{n-1}\|^2)\|\nabla u_j^{n+1}\|^2. \end{aligned}$$

Since $u_j \in L^\infty(0, T; H^1(\Omega))$, we have the estimates

$$\begin{aligned} -2b^*(\xi_{j,h}^n, u_j^{n+1}, \xi_{j,h}^{n+1}) &\le C\|\nabla \xi_{j,h}^n\|^{\frac{1}{2}}\|\xi_{j,h}^n\|^{\frac{1}{2}}\|\nabla u_j^{n+1}\|\|\nabla \xi_{j,h}^{n+1}\| \\ &\le C\|\nabla \xi_{j,h}^n\|^{\frac{1}{2}}\|\xi_{j,h}^n\|^{\frac{1}{2}}\|\nabla \xi_{j,h}^{n+1}\| \\ &\le C\Big(\epsilon\|\nabla \xi_{j,h}^{n+1}\|^2 + \frac{1}{\epsilon}\|\nabla \xi_{j,h}^n\|\|\xi_{j,h}^n\|\Big) \\ &\le C\Big(\epsilon\|\nabla \xi_{j,h}^{n+1}\|^2 + \frac{1}{\epsilon}\Big(\delta\|\nabla \xi_{j,h}^n\|^2 + \frac{1}{\delta}\|\xi_{j,h}^n\|^2\Big)\Big) \\ &\le C_0\overline{\nu}\|\nabla \xi_{j,h}^{n+1}\|^2 + C_0\overline{\nu}\|\nabla \xi_{j,h}^n\|^2 + CC_0^{-3}\overline{\nu}^{-3}\|\xi_{j,h}^n\|^2. \end{aligned} \tag{C.10}$$

Similarly,

$$\begin{aligned} b^*(\xi_{j,h}^{n-1}, u_j^{n+1}, \xi_{j,h}^{n+1}) &\le C\|\nabla \xi_{j,h}^{n-1}\|^{\frac{1}{2}}\|\xi_{j,h}^{n-1}\|^{\frac{1}{2}}\|\nabla u_j^{n+1}\|\|\nabla \xi_{j,h}^{n+1}\| \\ &\le C\|\nabla \xi_{j,h}^{n-1}\|^{\frac{1}{2}}\|\xi_{j,h}^{n-1}\|^{\frac{1}{2}}\|\nabla \xi_{j,h}^{n+1}\| \\ &\le C\Big(\epsilon\|\nabla \xi_{j,h}^{n+1}\|^2 + \frac{1}{\epsilon}\|\nabla \xi_{j,h}^{n-1}\|\|\xi_{j,h}^{n-1}\|\Big) \\ &\le C\Big(\epsilon\|\nabla \xi_{j,h}^{n+1}\|^2 + \frac{1}{\epsilon}\Big(\delta\|\nabla \xi_{j,h}^{n-1}\|^2 + \frac{1}{\delta}\|\xi_{j,h}^{n-1}\|^2\Big)\Big) \\ &\le C_0\overline{\nu}\|\nabla \xi_{j,h}^{n+1}\|^2 + C_0\overline{\nu}\|\nabla \xi_{j,h}^{n-1}\|^2 + CC_0^{-3}\overline{\nu}^{-3}\|\xi_{j,h}^{n-1}\|^2. \end{aligned} \tag{C.11}$$

Also by inequality (2.5) and the stability result (3.3), i.e. $\|u_{j,h}^n\|^2 \le C$, we have

$$\begin{aligned} -2b^*(u_{j,h}^n, \eta_j^{n+1}, \xi_{j,h}^{n+1}) &\le C\|\nabla u_{j,h}^n\|^{\frac{1}{2}}\|u_{j,h}^n\|^{\frac{1}{2}}\|\nabla \eta_j^{n+1}\|\|\nabla \xi_{j,h}^{n+1}\| \\ &\le C_0\overline{\nu}\|\nabla \xi_{j,h}^{n+1}\|^2 + \frac{C^2}{4C_0\overline{\nu}}\|\nabla u_{j,h}^n\|\|\nabla \eta_j^{n+1}\|^2, \end{aligned} \tag{C.12}$$

$$\begin{aligned} b^*(u_{j,h}^{n-1}, \eta_j^{n+1}, \xi_{j,h}^{n+1}) &\le C\|\nabla u_{j,h}^{n-1}\|^{\frac{1}{2}}\|u_{j,h}^{n-1}\|^{\frac{1}{2}}\|\nabla \eta_j^{n+1}\|\|\nabla \xi_{j,h}^{n+1}\| \\ &\le C_0\overline{\nu}\|\nabla \xi_{j,h}^{n+1}\|^2 + \frac{C^2}{4C_0\overline{\nu}}\|\nabla u_{j,h}^{n-1}\|\|\nabla \eta_j^{n+1}\|^2, \end{aligned} \tag{C.13}$$

$$\begin{aligned} -b^*(u_j^{n+1} - (2u_j^n - u_j^{n-1}), u_j^{n+1}, \xi_{j,h}^{n+1}) &\le C\|\nabla(u_j^{n+1} - 2u_j^n + u_j^{n-1})\|\|\nabla u_j^{n+1}\|\|\nabla \xi_{j,h}^{n+1}\| \\ &\le C_0\overline{\nu}\|\nabla \xi_{j,h}^{n+1}\|^2 + \frac{C^2}{4C_0\overline{\nu}}\|\nabla(u_j^{n+1} - 2u_j^n + u_j^{n-1})\|^2\|\nabla u_{j,h}^{n+1}\|^2 \\ &\le C_0\overline{\nu}\|\nabla \xi_{j,h}^{n+1}\|^2 + \frac{C^2}{4C_0\overline{\nu}}\Delta t^3\|\nabla u_j^{n+1}\|^2 \int_{t^{n-1}}^{t^{n+1}} \|\nabla u_{j,tt}\|^2\,dt. \end{aligned} \tag{C.14}$$

Now we bound the third nonlinear term in (C.2):

$$\begin{aligned} -b^*(u_{j,h}'^n, u_{j,h}^{n+1} - 2u_{j,h}^n + u_{j,h}^{n-1}, \xi_{j,h}^{n+1}) &= b^*(u_{j,h}'^n, e_j^{n+1} - 2e_j^n + e_j^{n-1}, \xi_{j,h}^{n+1}) - b^*(u_{j,h}'^n, u_j^{n+1} - 2u_j^n + u_j^{n-1}, \xi_{j,h}^{n+1}) \\ &= b^*(u_{j,h}'^n, \xi_{j,h}^{n+1} - 2\xi_{j,h}^n + \xi_{j,h}^{n-1}, \xi_{j,h}^{n+1}) + b^*(u_{j,h}'^n, \eta_j^{n+1} - 2\eta_j^n + \eta_j^{n-1}, \xi_{j,h}^{n+1}) \\ &\quad - b^*(u_{j,h}'^n, u_j^{n+1} - 2u_j^n + u_j^{n-1}, \xi_{j,h}^{n+1}). \end{aligned} \tag{C.15}$$

By skew symmetry,

$$-b^*(u'^n_{j,h}, \xi^{n+1}_{j,h} - 2\xi^n_{j,h} + \xi^{n-1}_{j,h}, \xi^{n+1}_{j,h}) = b^*(u'^n_{j,h}, \xi^{n+1}_{j,h}, \xi^{n+1}_{j,h} - 2\xi^n_{j,h} + \xi^{n-1}_{j,h}).$$

Using (2.6) and inverse inequality (2.4) gives

$$\begin{aligned} b^*(u'^n_{j,h}, 2\xi^n_{j,h} - \xi^{n-1}_{j,h} - \xi^{n+1}_{j,h}, \xi^{n+1}_{j,h}) &\le C\|\nabla u'^n_{j,h}\|\|\nabla \xi^{n+1}_{j,h}\|\|\nabla(\xi^{n+1}_{j,h} - 2\xi^n_{j,h} + \xi^{n-1}_{j,h})\|^{\frac{1}{2}}\|\xi^{n+1}_{j,h} - 2\xi^n_{j,h} + \xi^{n-1}_{j,h}\|^{\frac{1}{2}} \\ &\le C\|\nabla u'^n_{j,h}\|\|\nabla \xi^{n+1}_{j,h}\|(h^{-1/2})\|\xi^{n+1}_{j,h} - 2\xi^n_{j,h} + \xi^{n-1}_{j,h}\| \\ &\le \frac{1}{8\Delta t}\|\xi^{n+1}_{j,h} - 2\xi^n_{j,h} + \xi^{n-1}_{j,h}\|^2 + C\frac{\Delta t}{h}\|\nabla u'^n_{j,h}\|^2\|\nabla \xi^{n+1}_{j,h}\|^2, \end{aligned} \tag{C.16}$$

$$\begin{aligned} b^*(u'^n_{j,h}, \eta^{n+1}_j - 2\eta^n_j + \eta^{n-1}_j, \xi^{n+1}_{j,h}) &\le C\|\nabla u'^n_{j,h}\|\|\nabla(\eta^{n+1}_j - 2\eta^n_j + \eta^{n-1}_j)\|\|\nabla \xi^{n+1}_{j,h}\| \\ &\le C_0\overline{\nu}\|\nabla \xi^{n+1}_{j,h}\|^2 + CC_0^{-1}\overline{\nu}^{-1}\|\nabla u'^n_{j,h}\|^2\|\nabla(\eta^{n+1}_j - 2\eta^n_j + \eta^{n-1}_j)\|^2 \\ &\le C_0\overline{\nu}\|\nabla \xi^{n+1}_{j,h}\|^2 + \frac{C\Delta t^3}{C_0\overline{\nu}}\|\nabla u'^n_{j,h}\|^2 \int_{t^{n-1}}^{t^{n+1}} \|\nabla \eta_{j,tt}\|^2\,dt, \end{aligned} \tag{C.17}$$

$$\begin{aligned} b^*(u'^n_{j,h}, u^{n+1}_j - 2u^n_j + u^{n-1}_j, \xi^{n+1}_{j,h}) &\le C\|\nabla u'^n_{j,h}\|\|\nabla(u^{n+1}_j - 2u^n_j + u^{n-1}_j)\|\|\nabla \xi^{n+1}_{j,h}\| \\ &\le C_0\overline{\nu}\|\nabla \xi^{n+1}_{j,h}\|^2 + CC_0^{-1}\overline{\nu}^{-1}\|\nabla u'^n_{j,h}\|^2\|\nabla(u^{n+1}_j - 2u^n_j + u^{n-1}_j)\|^2 \\ &\le C_0\overline{\nu}\|\nabla \xi^{n+1}_{j,h}\|^2 + CC_0^{-1}\overline{\nu}^{-1}\Delta t^3\|\nabla u'^n_{j,h}\|^2 \int_{t^{n-1}}^{t^{n+1}} \|\nabla u_{j,tt}\|^2\,dt. \end{aligned} \tag{C.18}$$

For the pressure term in (C.2), since $\xi^{n+1}_{j,h} \in V_h$, we have

$$\begin{aligned} (p^{n+1}_j, \nabla\cdot\xi^{n+1}_{j,h}) &= (p^{n+1}_j - q^{n+1}_{j,h}, \nabla\cdot\xi^{n+1}_{j,h}) \\ &\le \sqrt{d}\,\|p^{n+1}_j - q^{n+1}_{j,h}\|\|\nabla\xi^{n+1}_{j,h}\| \\ &\le \frac{d}{4\,C_0}\overline{\nu}^{-1}\|p^{n+1}_j - q^{n+1}_{j,h}\|^2 + C_0\,\overline{\nu}\|\nabla\xi^{n+1}_{j,h}\|^2. \end{aligned} \tag{C.19}$$

The other terms are bounded as

$$\begin{aligned} \Big(\frac{3\eta^{n+1}_j - 4\eta^n_j + \eta^{n-1}_j}{2\Delta t}, \xi^{n+1}_{j,h}\Big) &\le \frac{C}{4C_0}\overline{\nu}^{-1}\Big\|\frac{3\eta^{n+1}_j - 4\eta^n_j + \eta^{n-1}_j}{2\Delta t}\Big\|^2 + C_0\overline{\nu}\|\nabla\xi^{n+1}_{j,h}\|^2 \\ &\le \frac{C}{4C_0}\overline{\nu}^{-1}\Big\|\frac{1}{\Delta t}\int_{t^{n-1}}^{t^{n+1}} \eta_{j,t}\,dt\Big\|^2 + C_0\overline{\nu}\|\nabla\xi^{n+1}_{j,h}\|^2 \\ &\le \frac{C}{4C_0\overline{\nu}\Delta t}\int_{t^{n-1}}^{t^{n+1}} \|\eta_{j,t}\|^2\,dt + C_0\overline{\nu}\|\nabla\xi^{n+1}_{j,h}\|^2 \end{aligned}$$

and

$$\begin{aligned} \mathrm{Intp}(u^{n+1}_j; \xi^{n+1}_{j,h}) &= \Big(\frac{3u^{n+1}_j - 4u^n_j + u^{n-1}_j}{2\Delta t} - u_{j,t}(t^{n+1}), \xi^{n+1}_{j,h}\Big) \\ &\le C\Big\|\frac{3u^{n+1}_j - 4u^n_j + u^{n-1}_j}{2\Delta t} - u_{j,t}(t^{n+1})\Big\|\|\nabla\xi^{n+1}_{j,h}\| \\ &\le C_0\overline{\nu}\|\nabla\xi^{n+1}_{j,h}\|^2 + \frac{C^2}{4C_0\overline{\nu}}\Big\|\frac{3u^{n+1}_j - 4u^n_j + u^{n-1}_j}{2\Delta t} - u_{j,t}(t^{n+1})\Big\|^2 \\ &\le C_0\overline{\nu}\|\nabla\xi^{n+1}_{j,h}\|^2 + \frac{5C^2\Delta t^3}{8C_0\overline{\nu}}\int_{t^{n-1}}^{t^{n+1}} \|u_{j,ttt}\|^2\,dt. \end{aligned} \tag{C.20}$$

Combining (C.3)–(C.20) and taking $C_0 = \frac{1}{17}\frac{\epsilon}{\sqrt{\mu}+\epsilon}(1-\frac{\sqrt{\mu}}{2})$ with $\epsilon \in (0, 2-2\sqrt{\mu})$, we have for all σ such that $0<\sigma<1$,

$$\begin{aligned}
&\frac{1}{4\Delta t}(\|\xi_{j,h}^{n+1}\|^2 + \|2\xi_{j,h}^{n+1} - \xi_{j,h}^{n}\|^2) - \frac{1}{4\Delta t}(\|\xi_{j,h}^{n}\|^2 + \|2\xi_{j,h}^{n} - \xi_{j,h}^{n-1}\|^2) + \frac{1}{8\Delta t}\|\xi_{j,h}^{n+1} - 2\xi_{j,h}^{n} + \xi_{j,h}^{n-1}\|^2 \\
&\quad + 2C_0\overline{\nu}(\|\nabla\xi_{j,h}^{n+1}\|^2 - \|\nabla\xi_{j,h}^{n}\|^2) + C_0\overline{\nu}(\|\nabla\xi_{j,h}^{n}\|^2 - \|\nabla\xi_{j,h}^{n-1}\|^2) \\
&\quad + \overline{\nu}\sigma\Big(1 - 17C_0 - \frac{3|\nu_j-\overline{\nu}|}{2\overline{\nu}}\Big)(\|\nabla\xi_{j,h}^{n+1}\|^2 - \|\nabla\xi_{j,h}^{n}\|^2) \\
&\quad + \overline{\nu}\Big((1-\sigma)\Big(1 - 17C_0 - \frac{3|\nu_j-\overline{\nu}|}{2\overline{\nu}}\Big) - \frac{C\Delta t}{\overline{\nu}h}\|\nabla u_{j,h}^{\prime n}\|^2\Big)\|\nabla\xi_{j,h}^{n+1}\|^2 \\
&\quad + \overline{\nu}\Big(\frac{2}{3}\sigma\Big(1 - 17C_0 - \frac{3|\nu_j-\overline{\nu}|}{2\overline{\nu}}\Big) - \frac{|\nu_j-\overline{\nu}|}{\overline{\nu}}\Big)\|\nabla\xi_{j,h}^{n}\|^2 \\
&\quad + \overline{\nu}\frac{\sigma}{3}\Big(1 - 17C_0 - \frac{3|\nu_j-\overline{\nu}|}{2\overline{\nu}}\Big)(\|\nabla\xi_{j,h}^{n}\|^2 - \|\nabla\xi_{j,h}^{n-1}\|^2) \\
&\quad + \overline{\nu}\Big(\frac{\sigma}{3}\Big(1 - 17C_0 - \frac{3|\nu_j-\overline{\nu}|}{2\overline{\nu}}\Big) - \frac{|\nu_j-\overline{\nu}|}{2\overline{\nu}}\Big)\|\nabla\xi_{j,h}^{n-1}\|^2 \\
&\leq CC_0^{-3}\nu^{-3}(\|\xi_{j,h}^{n}\|^2 + \|\xi_{j,h}^{n-1}\|^2) + \frac{C}{4C_0\overline{\nu}}\|\nabla u_{j,h}^{n}\|\|\nabla\eta_j^{n+1}\|^2 + \frac{C}{4C_0\overline{\nu}}\|\nabla u_{j,h}^{n-1}\|\|\nabla\eta_j^{n+1}\|^2 \\
&\quad + \frac{\Delta t^3}{4C_0}\frac{|\nu_j-\overline{\nu}|^2}{\overline{\nu}}\int_{t^{n-1}}^{t^{n+1}}\|\nabla u_{j,tt}\|^2\,dt + \frac{C\Delta t^3}{4C_0\overline{\nu}}\|\nabla u_j^{n+1}\|^2\int_{t^{n-1}}^{t^{n+1}}\|\nabla u_{j,tt}\|^2\,dt \\
&\quad + \frac{C}{4C_0\overline{\nu}}(\|\nabla\eta_j^{n}\|^2 + \|\nabla\eta_j^{n-1}\|^2)\|\nabla u_j^{n+1}\|^2 + \frac{C\Delta t^3}{C_0\overline{\nu}}\|\nabla u_{j,h}^{\prime n}\|^2\int_{t^{n-1}}^{t^{n+1}}\|\nabla u_{j,tt}\|^2\,dt \\
&\quad + \frac{C\Delta t^3}{C_0\overline{\nu}}\|\nabla u_{j,h}^{\prime n}\|^2\int_{t^{n-1}}^{t^{n+1}}\|\nabla\eta_{j,tt}\|^2\,dt + \frac{d}{4C_0\overline{\nu}}\|p_j^{n+1} - q_{j,h}^{n+1}\|^2 \\
&\quad + \frac{C}{4C_0\overline{\nu}\Delta t}\int_{t^{n-1}}^{t^{n+1}}\|\eta_{j,t}\|^2\,dt + \frac{\overline{\nu}}{4C_0}\|\nabla\eta_j^{n+1}\|^2 + \frac{1}{C_0}\frac{|\nu_j-\overline{\nu}|^2}{\overline{\nu}}\|\nabla\eta_j^{n}\|^2 \\
&\quad + \frac{1}{4C_0}\frac{|\nu_j-\overline{\nu}|^2}{\overline{\nu}}\|\nabla\eta_j^{n-1}\|^2 + \frac{C\Delta t^3}{4C_0\overline{\nu}}\int_{t^{n-1}}^{t^{n+1}}\|u_{j,ttt}\|^2\,dt,
\end{aligned} \tag{C.21}$$

where C on the right-hand side is a generic constant independent of Δt and h. Similar to the discussion in the stability proof, we take

$$\sigma = \frac{\sqrt{\mu}+\epsilon}{2-\sqrt{\mu}}.$$

By the viscosity deviation condition (3.2), we have

$$\begin{aligned}
1 - 17C_0 - \frac{3|\nu_j-\overline{\nu}|}{2\overline{\nu}} &= \frac{(2+\epsilon)\sqrt{\mu}}{2(\sqrt{\mu}+\epsilon)} - \frac{3|\nu_j-\overline{\nu}|}{2\overline{\nu}} > \frac{(2+\epsilon)\sqrt{\mu}}{2(\sqrt{\mu}+\epsilon)} - \frac{\sqrt{\mu}}{2} = \frac{\sqrt{\mu}(2-\sqrt{\mu})}{2(\sqrt{\mu}+\epsilon)} > 0, \\
\frac{2}{3}\sigma\Big(1 - 17C_0 - \frac{3|\nu_j-\overline{\nu}|}{2\overline{\nu}}\Big) - \frac{|\nu_j-\overline{\nu}|}{\overline{\nu}} &> \frac{2}{3}\frac{\sqrt{\mu}+\epsilon}{2-\sqrt{\mu}}\frac{\sqrt{\mu}(2-\sqrt{\mu})}{2(\sqrt{\mu}+\epsilon)} - \frac{\sqrt{\mu}}{3} = 0, \\
\frac{1}{3}\sigma\Big(1 - 17C_0 - \frac{3|\nu_j-\overline{\nu}|}{2\overline{\nu}}\Big) - \frac{|\nu_j-\overline{\nu}|}{2\overline{\nu}} &> 0.
\end{aligned}$$

Also, by the stability condition (3.2), we have

$$\begin{aligned}
(1-\sigma)\Big(1 - 17C_0 - \frac{3|\nu_j-\overline{\nu}|}{2\overline{\nu}}\Big) - \frac{C\Delta t}{\overline{\nu}h}\|\nabla u_{j,h}^{\prime n}\|^2 &= \frac{2-2\sqrt{\mu}-\epsilon}{2-\sqrt{\mu}}\frac{\sqrt{\mu}(2-\sqrt{\mu})}{2(\sqrt{\mu}+\epsilon)} - C\frac{\Delta t}{\overline{\nu}h}\|\nabla u_{j,h}^{\prime n}\|^2 \\
&> \frac{(2-2\sqrt{\mu}-\epsilon)\sqrt{\mu}}{2(\sqrt{\mu}+\epsilon)} - \frac{(2-2\sqrt{\mu}-\epsilon)\sqrt{\mu}}{2(\sqrt{\mu}+\epsilon)} = 0.
\end{aligned}$$

Then (C.21) reduces to

$$
\begin{aligned}
&\frac{1}{4\Delta t}(\|\xi_{j,h}^{n+1}\|^2 + \|2\xi_{j,h}^{n+1} - \xi_{j,h}^{n}\|^2) - \frac{1}{4\Delta t}(\|\xi_{j,h}^{n}\|^2 + \|2\xi_{j,h}^{n} - \xi_{j,h}^{n-1}\|^2) + \frac{1}{8\Delta t}\|\xi_{j,h}^{n+1} - 2\xi_{j,h}^{n} + \xi_{j,h}^{n-1}\|^2\\
&\qquad + C_1\overline{\nu}(\|\nabla\xi_{j,h}^{n+1}\|^2 - \|\nabla\xi_{j,h}^{n}\|^2) + C_2\overline{\nu}(\|\nabla\xi_{j,h}^{n}\|^2 - \|\nabla\xi_{j,h}^{n-1}\|^2)\\
&\le CC_0^{-3}\overline{\nu}^{-3}(\|\xi_{j,h}^{n}\|^2 + \|\xi_{j,h}^{n-1}\|^2) + \frac{C}{4C_0\overline{\nu}}\|\nabla u_{j,h}^{n}\|\|\nabla\eta_j^{n+1}\|^2 + \frac{C}{4C_0\overline{\nu}}\|\nabla u_{j,h}^{n-1}\|\|\nabla\eta_j^{n+1}\|^2\\
&\qquad + \frac{\Delta t^3}{4C_0}\frac{|\nu_j - \overline{\nu}|^2}{\overline{\nu}}\int_{t^{n-1}}^{t^{n+1}}\|\nabla u_{j,tt}\|^2\,dt + \frac{C\Delta t^3}{4C_0\overline{\nu}}\|\nabla u_j^{n+1}\|^2\int_{t^{n-1}}^{t^{n+1}}\|\nabla u_{j,tt}\|^2\,dt\\
&\qquad + \frac{C}{4C_0\overline{\nu}}(\|\nabla\eta_j^{n}\|^2 + \|\nabla\eta_j^{n-1}\|^2)\|\nabla u_j^{n+1}\|^2 + \frac{C\Delta t^3}{C_0\overline{\nu}}\|\nabla u_{j,h}'^{n}\|^2\int_{t^{n-1}}^{t^{n+1}}\|\nabla u_{j,tt}\|^2\,dt\\
&\qquad + \frac{C\Delta t^3}{C_0\overline{\nu}}\|\nabla u_{j,h}'^{n}\|^2\int_{t^{n-1}}^{t^{n+1}}\|\nabla\eta_{j,tt}\|^2\,dt + \frac{d}{4C_0\overline{\nu}}\|p_j^{n+1} - q_{j,h}^{n+1}\|^2\\
&\qquad + \frac{C}{4C_0\overline{\nu}\Delta t}\int_{t^{n-1}}^{t^{n+1}}\|\eta_{j,t}\|^2\,dt + \frac{\overline{\nu}}{4C_0}\|\nabla\eta_j^{n+1}\|^2 + \frac{1}{C_0}\frac{|\nu_j - \overline{\nu}|^2}{\overline{\nu}}\|\nabla\eta_j^{n}\|^2\\
&\qquad + \frac{1}{4C_0}\frac{|\nu_j - \overline{\nu}|^2}{\overline{\nu}}\|\nabla\eta_j^{n-1}\|^2 + \frac{C\Delta t^3}{4C_0\overline{\nu}}\int_{t^{n-1}}^{t^{n+1}}\|u_{j,ttt}\|^2\,dt,
\end{aligned}
\tag{C.22}
$$

where

$$
C_1 = 2C_0 + \sigma\Big(1 - 17C_0 - \frac{3|\nu_j - \overline{\nu}|}{2\overline{\nu}}\Big) \quad\text{and}\quad C_2 = C_0 + \frac{\sigma}{3}\Big(1 - 17C_0 - \frac{3|\nu_j - \overline{\nu}|}{2\overline{\nu}}\Big).
$$

Summing (C.22) from $n = 1$ to $N - 1$, multiplying both sides by Δt and absorbing constants gives

$$
\begin{aligned}
&\frac{1}{4}(\|\xi_{j,h}^{N}\|^2 + \|2\xi_{j,h}^{N} - \xi_{j,h}^{N-1}\|^2) + \sum_{n=1}^{N-1}\frac{1}{8}\|\xi_{j,h}^{n+1} - 2\xi_{j,h}^{n} + \xi_{j,h}^{n-1}\|^2 + C_1\overline{\nu}\Delta t\|\nabla\xi_{j,h}^{N}\|^2 + C_2\overline{\nu}\Delta t\|\nabla\xi_{j,h}^{N-1}\|^2\\
&\le \frac{1}{4}(\|\xi_{j,h}^{1}\|^2 + \|2\xi_{j,h}^{1} - \xi_{j,h}^{0}\|^2) + C_1\overline{\nu}\Delta t\|\nabla\xi_{j,h}^{1}\|^2 + C_2\overline{\nu}\Delta t\|\nabla\xi_{j,h}^{0}\|^2 + \frac{C\Delta t}{\overline{\nu}^3}\sum_{n=0}^{N-1}\|\xi_{j,h}^{n}\|^2\\
&\quad + C\Delta t\sum_{n=1}^{N-1}\Big\{\overline{\nu}^{-1}\|\nabla u_{j,h}^{n}\|\|\nabla\eta_j^{n+1}\|^2 + \overline{\nu}^{-1}\|\nabla u_{j,h}^{n-1}\|\|\nabla\eta_j^{n+1}\|^2 + \Delta t^3\frac{|\nu_j - \overline{\nu}|^2}{\overline{\nu}}\int_{t^{n-1}}^{t^{n+1}}\|\nabla u_{j,tt}\|^2\,dt\\
&\qquad + \Delta t^3\overline{\nu}^{-1}\|\nabla u_j^{n+1}\|^2\int_{t^{n-1}}^{t^{n+1}}\|\nabla u_{j,tt}\|^2\,dt + \overline{\nu}^{-1}(\|\nabla\eta_j^{n}\|^2 + \|\nabla\eta_j^{n-1}\|^2)\|\nabla u_j^{n+1}\|^2\\
&\qquad + \Delta t^3\overline{\nu}^{-1}\|\nabla u_{j,h}'^{n}\|^2\int_{t^{n-1}}^{t^{n+1}}\|\nabla u_{j,tt}\|^2\,dt + \Delta t^3\overline{\nu}^{-1}\|\nabla u_{j,h}'^{n}\|^2\int_{t^{n-1}}^{t^{n+1}}\|\nabla\eta_{j,tt}\|^2\,dt\\
&\qquad + \overline{\nu}^{-1}\|p_j^{n+1} - q_{j,h}^{n+1}\|^2 + \overline{\nu}^{-1}\Delta t^{-1}\int_{t^{n-1}}^{t^{n+1}}\|\eta_{j,t}\|^2\,dt + \overline{\nu}\|\nabla\eta_j^{n+1}\|^2\\
&\qquad + \frac{|\nu_j - \overline{\nu}|^2}{\overline{\nu}}\|\nabla\eta_j^{n}\|^2 + \frac{|\nu_j - \overline{\nu}|^2}{\overline{\nu}}\|\nabla\eta_j^{n-1}\|^2 + \Delta t^3\overline{\nu}^{-1}\int_{t^{n-1}}^{t^{n+1}}\|u_{j,ttt}\|^2\,dt\Big\}.
\end{aligned}
$$

Using the interpolation inequality (2.2) and the bound on the time average norm of $\nabla u_{j,h}^{n+1}$ obtained from a slightly changed stability analysis by, in (A.1), splitting out $\frac{1}{8}\alpha\overline{\nu}\Delta t\|\nabla u_{j,h}^{n+1}\|^2$ from the viscosity term on the left-hand side and modifying the first two terms on the right-hand side to be $\frac{1}{8}\alpha\overline{\nu}\Delta t\|\nabla u_{j,h}^{n+1}\|^2$ and $\frac{2\Delta t}{\alpha\overline{\nu}}\|f_j^{n+1}\|_{-1}^2$, i.e., $\Delta t\sum_{n=1}^{N-1}\|\nabla u_{j,h}^{n+1}\|^2 \le C$, we have

$$\begin{aligned}\overline{\nu}^{-1}\Delta t\sum_{n=1}^{N-1}\|\nabla u_{j,h}^{n}\|\|\nabla\eta_j^{n+1}\|^2 &\le \overline{\nu}^{-1}h^{2k}\Delta t\sum_{n=1}^{N-1}\|\nabla u_{j,h}^{n}\|\|u_j^{n+1}\|_{k+1}^2\\&\le \nu^{-1}h^{2k}\Big(\Delta t\sum_{n=1}^{N-1}\|u_j^{n+1}\|_{k+1}^4+\Delta t\sum_{n=1}^{N-1}\|\nabla u_{j,h}^{n}\|^2\Big)\\&\le \nu^{-1}h^{2k}|||u_j|||_{4,k+1}^4+C\nu^{-1}h^{2k},\\ \overline{\nu}^{-1}\Delta t\sum_{n=1}^{N-1}\|\nabla u_{j,h}^{n-1}\|\|\nabla\eta_j^{n+1}\|^2 &\le \overline{\nu}^{-1}h^{2k}\Delta t\sum_{n=1}^{N-1}\|\nabla u_{j,h}^{n-1}\|\|u_j^{n+1}\|_{k+1}^2\\&\le \nu^{-1}h^{2k}\Big(\Delta t\sum_{n=1}^{N-1}\|u_j^{n+1}\|_{k+1}^4+\Delta t\sum_{n=1}^{N-1}\|\nabla u_{j,h}^{n-1}\|^2\Big)\\&\le \nu^{-1}h^{2k}|||u_j|||_{4,k+1}^4+C\nu^{-1}h^{2k}.\end{aligned}$$

Because $u_j\in L^\infty(0,T;H^1(\Omega))$, we have $\|\nabla u_j^{n+1}\|^2\le C$. Using convergence condition (3.1) and applying interpolation inequalities (2.1), (2.2) and (2.3) gives

$$\begin{aligned}&\frac14(\|\xi_{j,h}^N\|^2+\|2\xi_{j,h}^N-\xi_{j,h}^{N-1}\|^2)+\sum_{n=1}^{N-1}\frac18\|\xi_{j,h}^{n+1}-2\xi_{j,h}^n+\xi_{j,h}^{n-1}\|^2+C_1\overline{\nu}\Delta t\|\nabla\xi_{j,h}^N\|^2+C_2\overline{\nu}\Delta t\|\nabla\xi_{j,h}^{N-1}\|^2\\&\le\frac14(\|\xi_{j,h}^1\|^2+\|2\xi_{j,h}^1-\xi_{j,h}^0\|^2)+C_1\overline{\nu}\Delta t\|\nabla\xi_{j,h}^1\|^2+C_2\overline{\nu}\Delta t\|\nabla\xi_{j,h}^0\|^2\\&\quad+C\bigg[\frac{\Delta t}{\overline{\nu}^3}\sum_{n=0}^{N-1}\|\xi_{j,h}^n\|^2+\overline{\nu}^{-1}h^{2k}|||u_j|||_{4,k+1}^4+\overline{\nu}^{-1}h^{2k}+\Delta t^4\frac{|\nu_j-\overline{\nu}|^2}{\overline{\nu}}\|\nabla u_{j,tt}\|_{2,0}^2\\&\qquad+\overline{\nu}^{-1}\Delta t^4\|u_{j,tt}\|_{2,0}^2+\overline{\nu}^{-1}h^{2k}|||u_j|||_{2,k+1}^2+h\Delta t^3\|\nabla u_{j,tt}\|_{2,0}^2\\&\qquad+h^{2k+1}\Delta t^3\|\nabla u_{j,tt}\|_{2,k+1}^2+\overline{\nu}^{-1}h^{2s+2}|||p_j|||_{2,s+1}^2+\overline{\nu}^{-1}h^{2k+2}\|u_{j,t}\|_{2,k+1}^2\\&\qquad+\overline{\nu}h^{2k}|||u_j|||_{2,k+1}^2+\frac{|\nu_j-\overline{\nu}|^2}{\overline{\nu}}h^{2k}|||u_j|||_{2,k+1}^2+\overline{\nu}^{-1}\Delta t^4\|\nabla u_{j,ttt}\|_{2,0}^2\bigg].\end{aligned}$$

The next step uses an application of the discrete Gronwall inequality (Girault and Raviart [4, p. 176]):

$$\begin{aligned}&\frac14(\|\xi_{j,h}^N\|^2+\|2\xi_{j,h}^N-\xi_{j,h}^{N-1}\|^2)+\sum_{n=1}^{N-1}\frac18\|\xi_{j,h}^{n+1}-2\xi_{j,h}^n+\xi_{j,h}^{n-1}\|^2+C_1\overline{\nu}\Delta t\|\nabla\xi_{j,h}^N\|^2+C_2\overline{\nu}\Delta t\|\nabla\xi_{j,h}^{N-1}\|^2\\&\le e^{\frac{CT}{\overline{\nu}^3}}\bigg\{\frac14(\|\xi_{j,h}^1\|^2+\|2\xi_{j,h}^1-\xi_{j,h}^0\|^2)+C_1\overline{\nu}\Delta t\|\nabla\xi_{j,h}^1\|^2+C_2\overline{\nu}\Delta t\|\nabla\xi_{j,h}^0\|^2\\&\quad+C\bigg[\overline{\nu}^{-1}h^{2k}|||u_j|||_{4,k+1}^4+\overline{\nu}^{-1}h^{2k}+\Delta t^4\frac{|\nu_j-\overline{\nu}|^2}{\overline{\nu}}\|\nabla u_{j,tt}\|_{2,0}^2+\overline{\nu}^{-1}\Delta t^4\|u_{j,tt}\|_{2,0}^2+\overline{\nu}^{-1}h^{2k}|||u_j|||_{2,k+1}^2\\&\qquad+h\Delta t^3\|\nabla u_{j,tt}\|_{2,0}^2+h^{2k+1}\Delta t^3\|\nabla u_{j,tt}\|_{2,k+1}^2+\overline{\nu}^{-1}h^{2s+2}|||p_j|||_{2,s+1}^2+\overline{\nu}^{-1}h^{2k+2}\|u_{j,t}\|_{2,k+1}^2\\&\qquad+\overline{\nu}h^{2k}|||u_j|||_{2,k+1}^2+\frac{|\nu_j-\overline{\nu}|^2}{\overline{\nu}}h^{2k}|||u_j|||_{2,k+1}^2+\overline{\nu}^{-1}\Delta t^4\|\nabla u_{j,ttt}\|_{2,0}^2\bigg]\bigg\}.\end{aligned}\tag{C.23}$$

Recall that $e_j^n=\eta_j^n+\xi_{j,h}^n$. Using the triangle inequality on the error equation to split the error terms into the terms of η_j^n and $\xi_{j,h}^n$ gives

$$\frac14\|e_j^N\|^2+C_1\overline{\nu}\Delta t\|\nabla e_j^N\|^2\le\frac14\|\xi_{j,h}^N\|^2+C_1\overline{\nu}\Delta t\|\nabla\xi_{j,h}^N\|^2+\frac14\|\eta_j^N\|^2+C_1\overline{\nu}\Delta t\|\nabla\eta_j^N\|^2,$$

and

$$\begin{aligned}&\frac14(\|\xi_{j,h}^1\|^2+\|2\xi_{j,h}^1-\xi_{j,h}^0\|^2)+C_1\overline{\nu}\Delta t\|\nabla\xi_{j,h}^1\|^2+C_2\overline{\nu}\Delta t\|\nabla\xi_{j,h}^0\|^2\\&\le\frac14(\|e_j^1\|^2+\|2e_j^1-e_j^0\|^2)+C_1\overline{\nu}\Delta t\|\nabla e_j^1\|^2+C_2\overline{\nu}\Delta t\|\nabla e_j^0\|^2\\&\qquad+\frac14(\|\eta_j^1\|^2+\|2\eta_j^1-\eta_j^0\|^2)+C_1\overline{\nu}\Delta t\|\nabla\eta_j^1\|^2+C_2\overline{\nu}\Delta t\|\nabla\eta_j^0\|^2.\end{aligned}$$

Applying inequality (C.23), using the previous bounds for the η_j^n terms, and absorbing constants into a new constant C, we have Theorem 4.2. □

Funding: This research was partially supported by the U.S. Department of Energy under grants DE-SC0009324 and DE-SC0016540, the U.S. Air Force Office of Scientific Research grant FA9550-15-1-0001, a Defense Advanced Projects Agency contract administered under the Oak Ridge National Laboratory subcontract 4000145366, the U.S. National Science Foundation grants DMS-1522672 and DMS-1720001, and a University of Missouri Research Board grant.

References

[1] L. C. Berselli, On the large eddy simulation of the Taylor–Green vortex, *J. Math. Fluid Mech.* **7** (2005), no. 2, S164–S191.
[2] S. C. Brenner and L. R. Scott, *The Mathematical Theory of Finite Element Methods*, 3rd ed., Texts Appl. Math. 15, Springer, New York, 2008.
[3] G. J. Fix, M. D. Gunzburger and J. S. Peterson, On finite element approximations of problems having inhomogeneous essential boundary conditions, *Comput. Math. Appl.* **9** (1983), 687–700.
[4] V. Girault and P.-A. Raviart, *Finite Element Approximation of the Navier–Stokes Equations*, Lecture Notes in Math. 749, Springer, Berlin, 1979.
[5] A. Green and G. Taylor, Mechanism of the production of small eddies from larger ones, *Proc. Royal Soc. Lond. Ser. A Math. Phys. Sci.* **158** (1937), 499–521.
[6] J.-L. Guermond and L. Quartapelle, On stability and convergence of projection methods based on pressure Poisson equation, *Internat. J. Numer. Methods Fluids* **26** (1998), no. 9, 1039–1053.
[7] M. D. Gunzburger, *Finite Element Methods for Viscous Incompressible Flows*, Comput. Sci. Sci. Computing, Academic Press, Boston, 1989.
[8] M. Gunzburger, N. Jiang and M. Schneier, A higher-order ensemble/proper orthogonal decomposition method for the nonstationary Navier–Stokes equations, *Int. J. Numer. Anal. Model.*, to appear; https://arxiv.org/abs/1709.06422.
[9] M. Gunzburger, N. Jiang and M. Schneier, An ensemble-proper orthogonal decomposition method for the nonstationary Navier–Stokes equations, *SIAM J. Numer. Anal.* **55** (2017), no. 1, 286–304.
[10] M. Gunzburger, N. Jiang and Z. Wang, An efficient algorithm for simulating ensembles of parameterized flow problems, preprint (2017), https://arxiv.org/abs/1705.09350.
[11] Y. He, Two-level method based on finite element and Crank–Nicolson extrapolation for the time-dependent Navier–Stokes equations, *SIAM J. Numer. Anal.* **41** (2003), no. 4, 1263–1285.
[12] Y. He, The Euler implicit/explicit scheme for the 2D time-dependent Navier–Stokes equations with smooth or non-smooth initial data, *Math. Comp.* **77** (2008), no. 264, 2097–2124.
[13] Y. He and W. Sun, Stability and convergence of the Crank–Nicolson/Adams–Bashforth scheme for the time-dependent Navier–Stokes equations, *SIAM J. Numer. Anal.* **45** (2007), no. 2, 837–869.
[14] J. G. Heywood and R. Rannacher, Finite-element approximation of the nonstationary Navier–Stokes problem. IV. Error analysis for second-order time discretization, *SIAM J. Numer. Anal.* **27** (1990), no. 2, 353–384.
[15] N. Jiang, A higher order ensemble simulation algorithm for fluid flows, *J. Sci. Comput.* **64** (2015), no. 1, 264–288.
[16] N. Jiang, A second-order ensemble method based on a blended backward differentiation formula timestepping scheme for time-dependent Navier–Stokes equations, *Numer. Methods Partial Differential Equations* **33** (2017), no. 1, 34–61.
[17] N. Jiang, S. Kaya and W. Layton, Analysis of model variance for ensemble based turbulence modeling, *Comput. Methods Appl. Math.* **15** (2015), no. 2, 173–188.
[18] N. Jiang and W. Layton, An algorithm for fast calculation of flow ensembles, *Int. J. Uncertain. Quantif.* **4** (2014), no. 4, 273–301.
[19] N. Jiang and W. Layton, Numerical analysis of two ensemble eddy viscosity numerical regularizations of fluid motion, *Numer. Methods Partial Differential Equations* **31** (2015), no. 3, 630–651.
[20] H. Johnston and J.-G. Liu, Accurate, stable and efficient Navier–Stokes solvers based on explicit treatment of the pressure term, *J. Comput. Phys.* **199** (2004), no. 1, 221–259.
[21] W. Layton, *Introduction to the Numerical Analysis of Incompressible Viscous Flows*, Comput. Sci. Eng. 6, Society for Industrial and Applied Mathematics, Philadelphia, 2008.
[22] M. Marion and R. Temam, Navier–Stokes equations: Theory and approximation, in: *Handbook of Numerical Analysis. VI*, North-Holland, Amsterdam (1998), 503–688.
[23] M. Mohebujjaman and L. G. Rebholz, An efficient algorithm for computation of MHD flow ensembles, *Comput. Methods Appl. Math.* **17** (2017), no. 1, 121–137.
[24] A. Takhirov, M. Neda and J. Waters, Time relaxation algorithm for flow ensembles, *Numer. Methods Partial Differential Equations* **32** (2016), no. 3, 757–777.
[25] F. Tone, Error analysis for a second order scheme for the Navier–Stokes equations, *Appl. Numer. Math.* **50** (2004), no. 1, 93–119.